REPUBLIC OF TURKEY

ALTINBAŞ UNIVERSITY

Institute of Graduate Studies

Electrical and Computer Engineering

WIND TURBINE ENERGY SYSTEM CONTROL WITH PARTICLE SWARM OPTIMIZATION

Moner ELMARYOL

Master of Science

Supervisor

Prof. Dr. Galip CANSEVER

Istanbul, 2022

WIND TURBINE ENERGY SYSTEM CONTROL WITH PARTICLE SWARM OPTIMIZATION

Moner ELMARYOL

Electrical and Computer Engineering

Master of Science

ALTINBAS UNIVERSITY

2022

The thesis/dissertation titled “WIND TURBINE ENERGY SYSTEM CONTROL WITH PARTICLE SWARM OPTIMIZATION” prepared by MONER ELMARYOL and submitted on 28 February 2022 has been **accepted by majority of votes** for the degree of Master of Arts/Master of Science/PhD in Electrical and Computer Engineering.

Prof. Dr. Galip CANSEVER

Supervisour

Thesis Defenese Jury Members:

Prof.Dr. Galip CANSEVER	Faculty of Engineering and Architecture, Altinbas University
Asst. Prof.Dr. Sefer KURNAZ	Faculty of Engineering and Architecture, Altinbas University
Asst. Prof.Dr. Serdar KARGIN	Faculty of Engineering and Architecture, Beykent University

I hereby declare that this thesis meets all format and submission requirements of a Master’s thesis

Submission date of the thesis to the Graduate Education Institute:____/___/____

I hereby declare that all information/data presented in this graduation project has been obtained in full accordance with academic rules and ethical conduct. I also declare all unoriginal materials and conclusions have been cited in the text and all references mentioned in the Reference List have been cited in the text, and vice versa as required by the abovementioned rules and conduct.

Moner ELMARYOL

ABSTRACT

WIND TURBINE ENERGY SYSTEM CONTROL WITH PARTICLE SWARM OPTIMIZATION

Elmaryol, Moner

M.Sc. Electrical and Computer Engineering ,Altınbas University,

Supervisor: Professor Dr. Galip CANSEVER

Date: February/2022

Pages: 60

Nowadays, the use of green energy is now more important in the world. Wind power is one of these green renewable energies and is a serious competitor of fossil fuel for electricity market. Also, the cost of production should be comparable to fossil fuels and other fuels in this competition. Infrastructure and machinery are of first importance for capital investment. For example, turbine design is an important factor that reduces energy costs, so as it can be understood, construction and operation are important factors that make wind energy competitive. The air flow of the wind and its mathematics are significant for understanding operating efficiency of wind turbine in a specific area because it leads to optimize and help for enhancing these control algorithms for inspection. The modeling has affected the change in the performance of the wind turbine. This thesis aims to model the wind turbine by examining the general information and these parameters in the light of the power coefficient factor. The coherent model results obtained from here aim to reduce production costs and become economical by helping designers and new generation turbine researchers to design and optimize these turbines.

Keywords: Wind Turbine Energy System, Control, Particle Swarm Optimization

TABLE OF CONTENTS

Pages

LIST OF TABLES

Pages

LIST OF FIGURES

Page

ABBREVIATIONS

PSO	:	Particle Swarm Optimization
HAWT	:	Horizontal Axis Wind Turbine
VAWT	:	Vertical Axis Wind Turbine
GA	:	Genetic Algorithm
GWO	:	Grey Wolf Optimization
PIC	:	Proportional Integral Controller
P	:	Proportional
PID	:	Proportional Integral Derivative

1. INTRODUCTION

1.1 BACKGROUND

Nowadays, people chose to consume renewable energy in life. Such as, wind power. Thanks to the power of wind, people achieve to access electricity or mechanical power. Manufacturing electricity from wind force that is an eco-friendly source and becoming more and more demanding from all around the world. The other sources which are non-renewable energy sources, such as fossil fuels, give damage to the environment due to the emitting hazardous gazes which also speed up the time of global warning. The way of producing electricity from wind force depends on 3 main devices which are basically altering the wind force into the electricity. The first device is rotor which is formed from 3 or fiber glass blades that connected to the hub which includes hydraulics motors which alter each blade according to preevailing wind condition, thus turbine is able to function effectively at varying wind speeds. The terms wind power plant or wind turbine or wind power converter are also used colloquially. Wind turbines are by far the most important form of using wind energy today [1][2][3]. In the middle of the 20th century, oil was valued in an unstable structure, but towards the end of the 20th century, in addition to increasing several times due to political crises, it also became a political pressure. The need for a new, clean, sustainable energy source arose when environmental effects and the increasing world population were added. Considering that it has also been used for mechanical purposes such as sailing ships in the past, reusing wind energy promised a better future in terms of energy production. However, serious work was required to achieve this. In the middle of the 20th century, the work of scientists such as Poul la Cour, Albert Betz, Palmer Putnam and Percy Thomas laid the foundations for this need. But in the early days, using wind energy had a higher cost than fossil fuels. The use of wind energy has gradually increased as the government support for R&D and tests started under the leadership of countries such as the USA, Germany and Denmark, and today, other states have increased their initiatives in this regard.

1.2 ADVANTAGES OF WIND ENERGY

One of the advantages of wind energy is that it blows faster in winter and generates more electricity when we need more electricity. This energy has an endless energy source and tested technology without causing pollution. Recent advances in industry have always reduced the cost of electricity generated by wind turbines; This is less than the cost of electricity generated by coal and nuclear fission, and is economically competitive. Also, like other renewable and sustainable energies, it does not have many opponents. Britain has a good position in terms of wind source in Europe. Denmark supplies 3.7% (600 million watts) of wind energy compared to the United Kingdom, which supplies only 25% of its electricity needs; If the UK wind source is 28 times higher than Denmark [4].

1.3 WIND ENERGY DISADVANTAGES

One of the biggest obstacles to using wind energy in Britain is said to be its environmental impact. Many people say that wind turbines are visually unpleasant and noisy; Especially because they are located in beautiful areas outside urban areas. But it must be said that a coal-fired generator will certainly be noisier and uglier than wind turbines. The constant sound of wind turbine turbines is an important issue for those who are close to them. The sound of these generators can now be controlled with the help of three-blade gears and turbines [5].

1.4 TYPES OF WIND TURBINES

As seen in Figure 1.1, wind turbines are generally classified according to axis, speed, power, number of blades, wind effect, gear characteristics, and installation locations.

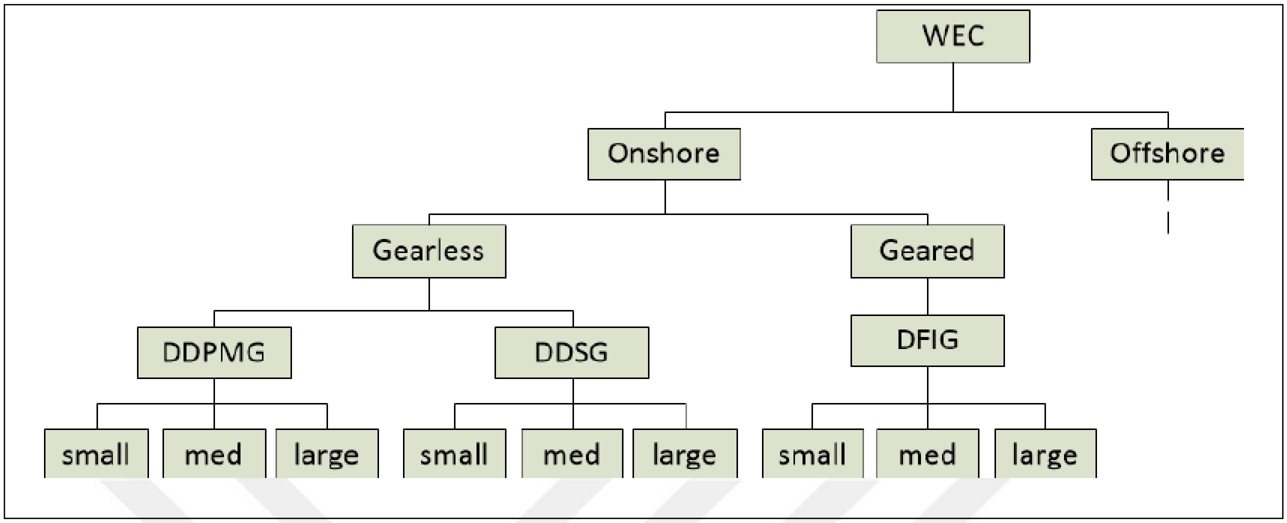

Figure 1.1: Classification of Wind turbines [6]

Wind turbines whose pivot of turn is corresponding to the breeze stream are called flat hub wind turbines, while wind turbines whose hub of revolution is opposite to the breeze stream are called vertical hub wind turbines.

In addition to the wind turbine type, the number of blades is the most important parameters effecting the power coefficient showing wind turbine performance. Considering the studies with different blade numbers of both horizontal and vertical wind turbine types, 3-bladed common wind turbines in horizontal axis wind turbines are the ones with the highest efficiency as seen in Figure 1.2. In addition, Savonius type vertical axis wind turbines with 2 blades and Darrieus type wind turbines with 3 blades are commonly used [7].

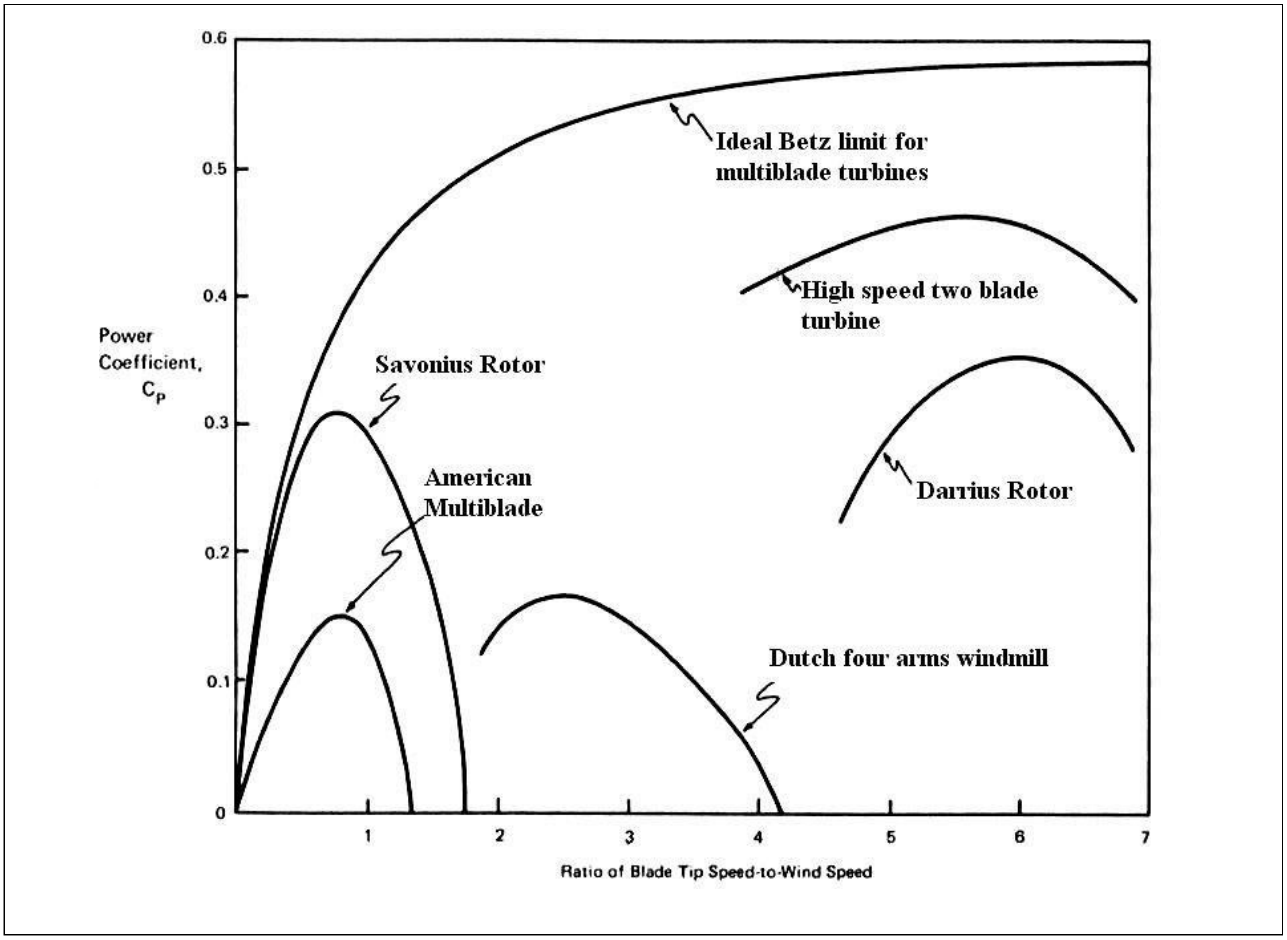

Figure 1.2: Betz's Law and Curve of performance of wind turbine types [8]

1.5 HORIZONTAL AXIS WIND TURBINES

Horizontal axis wind turbines are the type of wind turbine that can reach the highest power coefficient.

They generate power with the lift force obtained from the wind. As seen in Figure 1.3, structurally, horizontal axis wind turbines have a casing positioned on a tower, where the rotation axis of the turbine is aligned, and there are hubs and blades attached to the hub at the end. While the axis of rotation is positioned parallel to the air flow, the blades positioned perpendicular to the axis of rotation are also perpendicular to the air flow. As the propeller blades rotate, the shaft connected to the hub also rotates, the gearbox is placed opposite the shaft to adjust the speed, and the shaft rotating at the determined speed after the gearbox drives a generator.

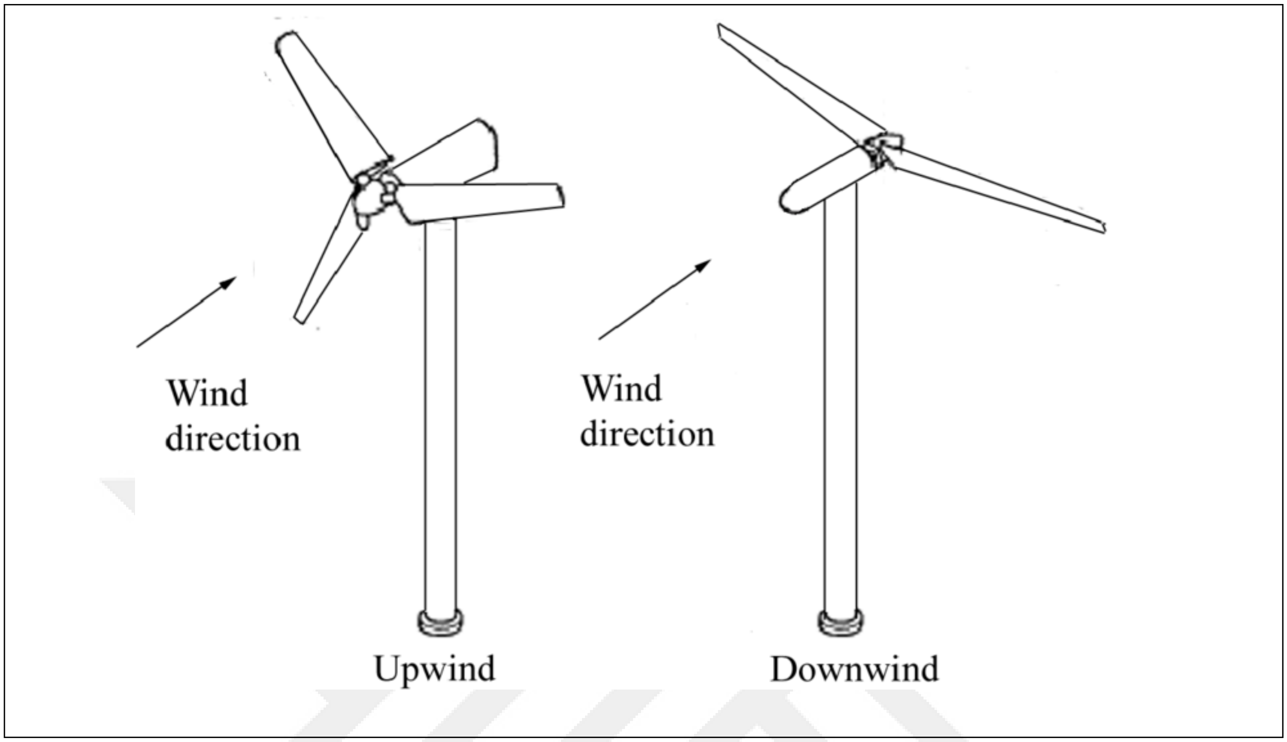

Figure 1.3: Horizontal Axis Wind turbine [9]

Thus, the cycle of converting wind energy to electrical energy has been completed and the obtained electrical energy is offered to industrial use by means of a transformer. Horizontal axis wind turbines cannot always meet the wind that can blow at an angle of 360˚ vertically. For this, a mechanism or a tail positioned on top of the enclosure as seen in figure 1.4 is used.

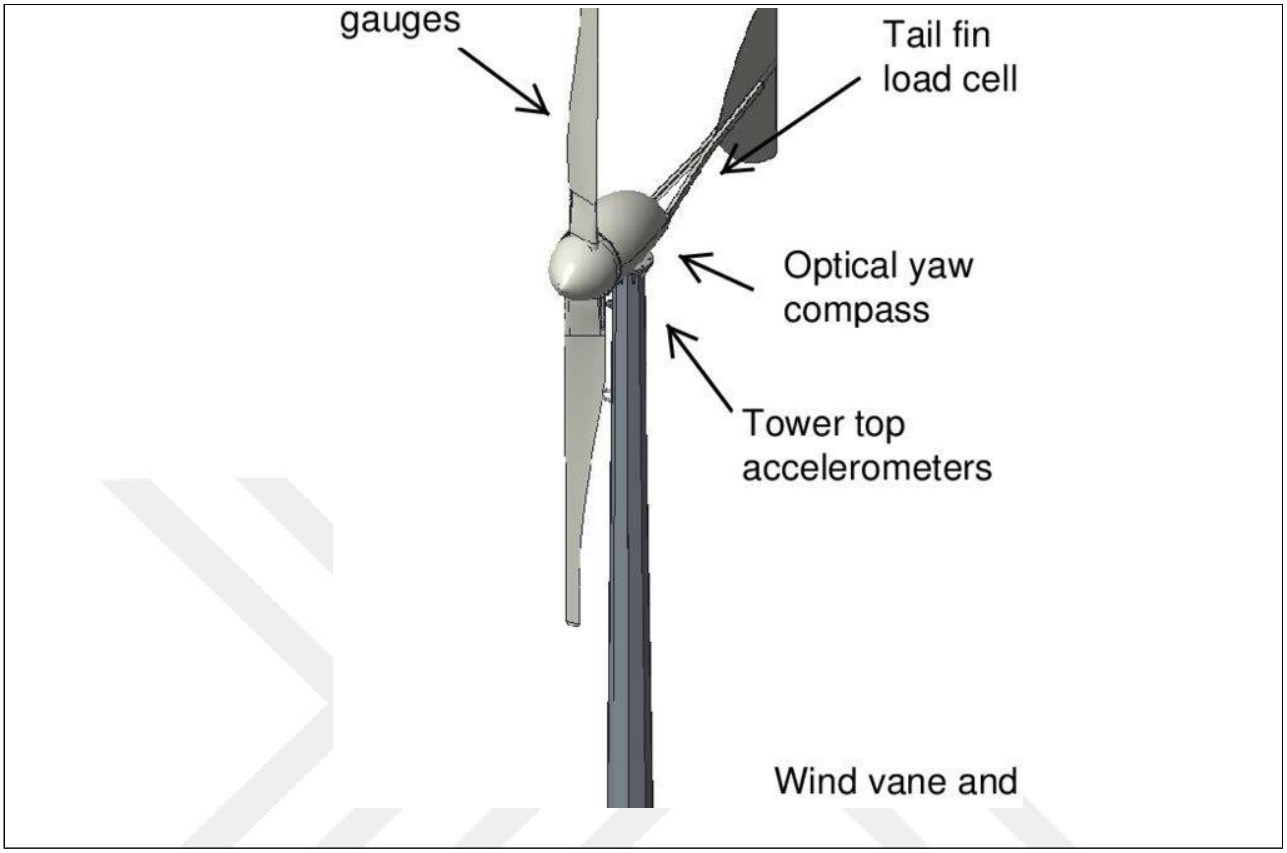

Figure 1.4: Tail Use in Horizontal axis wind turbine [10]

1.6 VERTICAL AXIS WIND TURBINES

Vertical axis wind turbines are wind turbines with the axis of rotation perpendicular to the air flow. There are types that generate power with the lift and drag force they get from the wind. The type that generates power by drag force is called Savonius type wind turbine. As seen in Figure 1.5, Savonius type wind turbines are formed when a barrel is cut in half along its vertical axis and two semi-cylindrical scoops are formed, with the open parts of the two scoops positioned in opposite directions from the center, again facing each other.

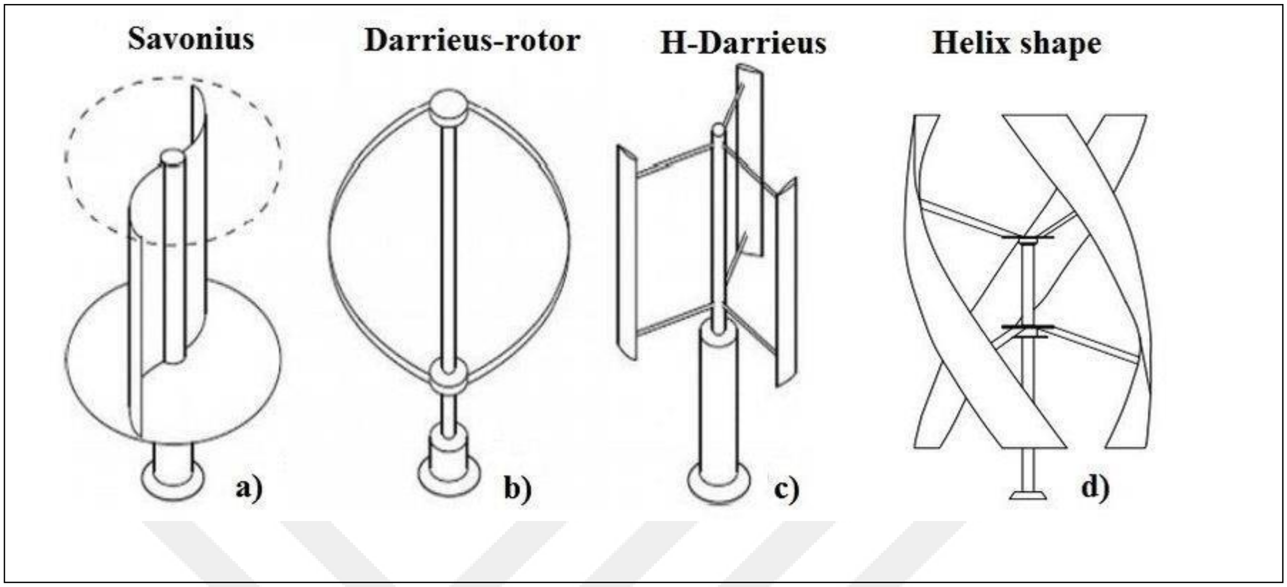

Figure 1.5: Savonius Type wind turbine [11]

Although Savonius type wind turbines are more advantageous in terms of starting their first motion, they lag behind Darrieus type wind turbines in terms of maximum power coefficient they can produce. As seen in Figure 1.6, Darrieus type wind turbines operate based on the principle that the high-pressure region of the airfoil exposed to the air flow, which has a shorter side, creates a lift force as a result of the application of force due to the pressure difference towards the low-pressure region, which is also called the intake surface with the longer side.

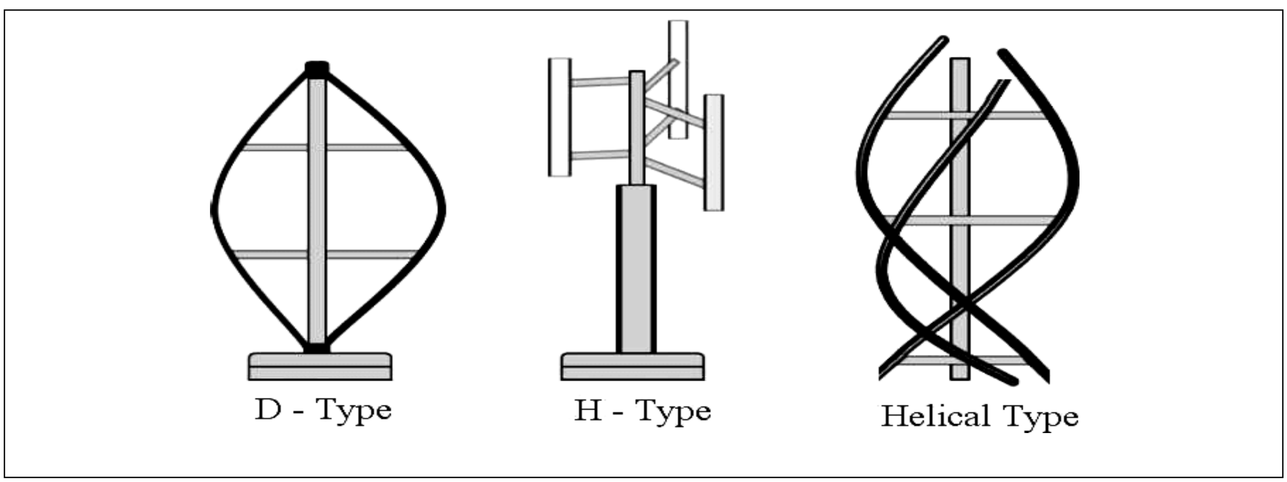

Figure 1.6: Darrieus Type wind turbine [12]

Although they need higher speed wind than Savonius type wind turbines to start the first movement, they can reach higher power coefficients than Savonius type wind turbines as power coefficient. In some applications, Savonius and Darrieus are used together. In this type of applications, Savonius type wind turbines take advantage of the initial advantage, while Darrieus type wind turbines can reach higher power coefficients after the turbine starts to operate. In general, although vertical axis wind turbines remain at lower power coefficients than horizontal axis wind turbines, they are more advantageous in terms of not needing an additional mechanism for the blades to take the wind upright, and having lower installation and maintenance costs.The main wind energy system components being a role to the future generations which are established a group and the group divided into different models.

1.7 THESIS ORGANIZATION

We have organized this thesis as Chapter 2 includes a review on literature review for methods that used in the thesis. Chapter 3 describes the particle swarm optimization method and illustrates the methods and analysis on the model. In Chapter 4, the proposed algorithm has been presented for a proposed system and analyzed, and then Chapter 5 discusses the conclusions and future scope for research.

2. WIND TURBINE SPECIFICATIONS

2.1 WIND TURBINE

Wind turbine made of blades these mounted on rotor which connected to nacelle and also connected to one or more electric motors. The gearbox enables the turbine connected to this electric motor to rotate at higher or lower revs according to the incoming wind speed. The system controls the electricity generation of the shaft connected to the electric motor with the help of a control unit. In addition, wind turbines come in two different designs. These classifications are made according to the axis the turbine rotates. Horizontal and Vartical axis wind turbine (HAWT and- VAWT). The VAWT's another name is Darrieous, which is the name of its inventor. An important feature of HAWT is that a day or a season can collect the maximum wind energy and adjust its blades for possible storms. Wind turbines can have fixed or variable rotation speeds and therefore have two different modes. A turbine rotating at a constant speed, rotates at a constant angular velocity independent of wind speed. The cost is less in this mode as there are no electronics such as inverters and converters. However, on the other hand, the disadvantage is that the turbine exposed to high wind speeds cannot rotate at its highest speed. Therefore, fixed-speed turbines generate less electrical energy at various wind speeds than turbines rotating at variable speeds, due to the changing fan speed according to the situation [13].

The power and torque generated by the wind turbine depends on several different factors. These are (1) turbine speed, (2) Bending of the rotor blade , (3) pitch angle of rotor blade , (4) turbin's shape and size , (5) turbine's area , (6) Rotor engineering; and also the (7) wind speed for both HAWT and VAWT. The link between these values and power generation plays an important role in the mathematical of turbin's model. The mathematical model of the wind is important for learning behavior of the turbine against it. Therefore, modeling for the region where it works affects the performance of the wind turbine. This article aims to examine all these criteria and modeling that affects performance. A typical modern wind turbine structure is shown in figure 2.1.

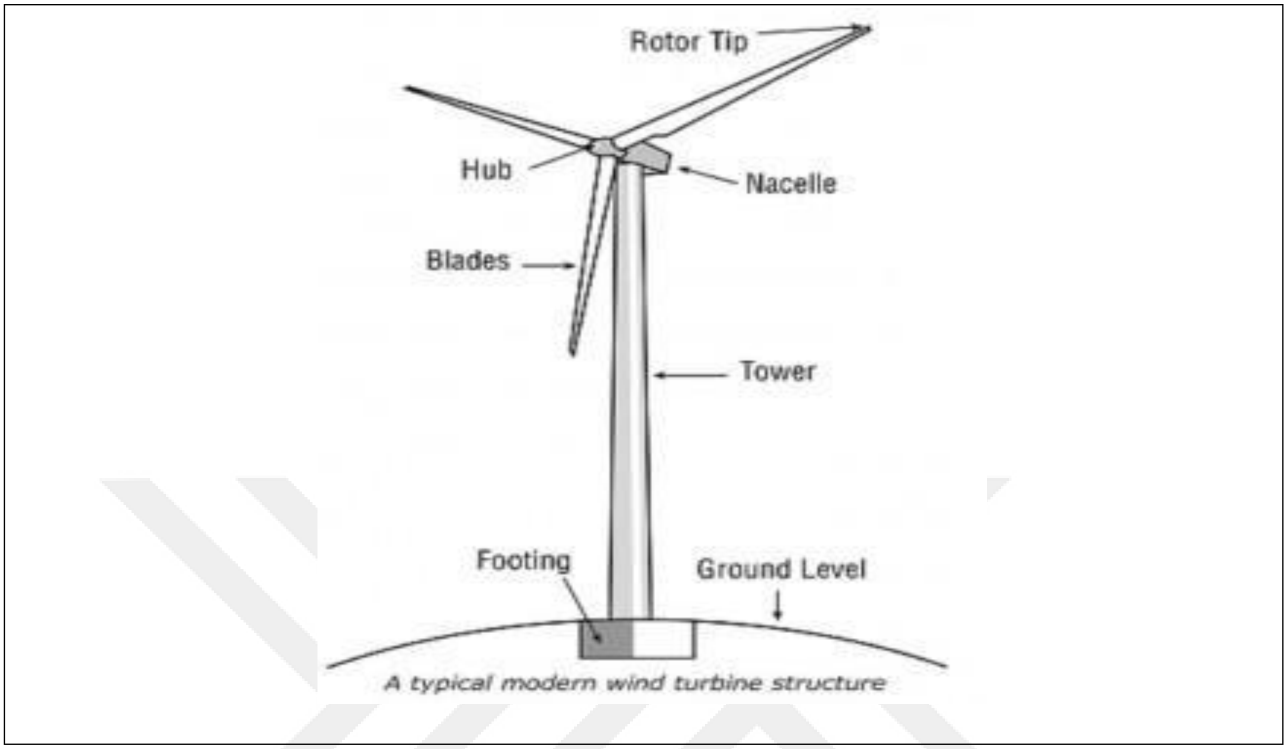

Figure 2.1: A typical Modern wind turbine structure

$$F = ma \quad (2.1)$$

that is why, the kinetic energy becomes

$$E = mas \quad (2.2)$$

What we learned from the kinematics of solid motion, v2 = u2 + 2as where u is the inside velocity of an object. This stands for that $a = \frac{v^2-u^2}{2s}$. Thinking the initial velocity of an object is void, we got that a = v2/2s. That is why from equation (2.2) we conclude

$$E=1/2mv2 \quad (2.3)$$

The kinetic energy formula is made by the truth which the mass of solid is permanent. At the other hand, if we take a look in wind as an aqua, density and velocity are not stable, and they can change that is why no constant mass for wind. Because of that Reeccab et. Al [10] produce the kinetic power law with factor of 4/6 besides 0.5 . In the report I should think that the wind density of does not change tremendously though with the difference in the rise of temperature and law of kinetic power should be involed from equation (2.3). That is why kinetic energy (joules) in wind of mass moving the velocity v. w. (wind) can be measured from equation (3) upside. power P for the wind has been got by change of rate of the kinetic power, i.e.

$$P = \frac{dE}{dt} = \frac{1}{2}\frac{dm}{dt}v_w^2 \qquad (2.4)$$

Although the flow rate of the mass dm/dt has been given by dm/dt = ρAvw where A is area over that the wind with this kind of a situation is flowing and density of the air is ρ. With the statement, Anderson and Bose [15] claim that the next experimental relation for Cp:

$$C_p = \frac{1}{2}(\lambda - 0.022\theta^2 - 5.6)e^{-0.17\lambda} \qquad (2.5)$$

As we understand, the power generated by a turbine depends on several different criteria such as the area of the rotor blades, the rotation of the blades' speed and the power parameter. Therefore, the amount of output power can be increased or decreased by changing the area and flow criteria, and this is actually the operating logic of the control system. Cp value is specific to the turbine design and it is a certain λ value. Equations of the model turbine (2.5) are power in the wind, power took by turbine, speed percentage of the turbine and the power parameter. Accordingly, the power output of wind power relies upon the parameters of these equations. It is not possible to control wind turbines rotating at constant speed. On the other hand, wind turbines rotating at variable speed can use generator torque to optimize power output. In addition, wind turbines rotating above the projected wind speed use the pitch control to adjust the power output. MATLAB should be used to analyze the change of cp versus λ. Consequently, changing θ and curves are obtained, these curves are simulated for the best performance of the turbine. The Simulated Power Coefficient is shown in fig 2.2.

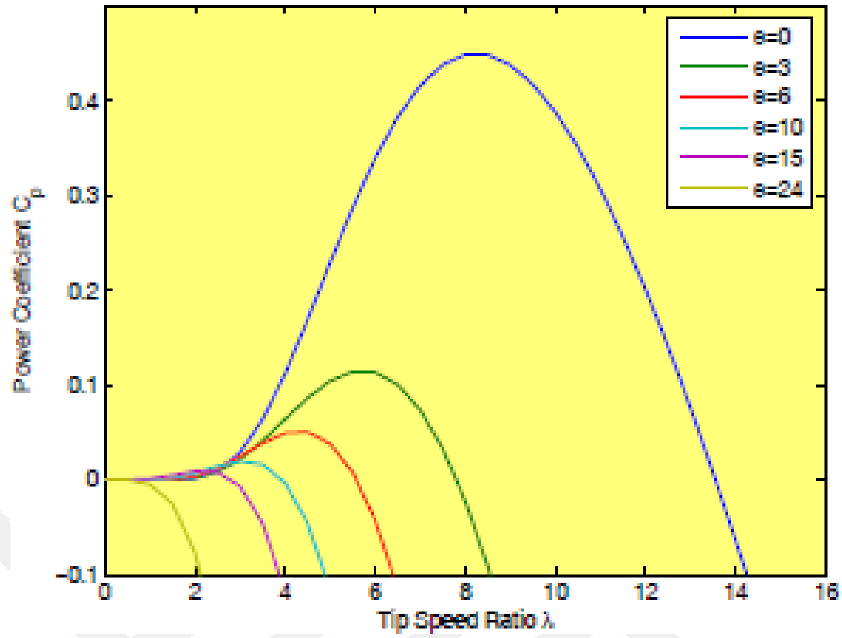

Figure 2.2: Simulated POWER Coefficient

The Modern (2013) wind turbine of the 3 MW class is shown in figure 2.3.

Figure 2. 3: Modern (2013) Wind turbine of the 3 MW class

2.2 CHARACTERISTIC FEATURES OF WIND TURBINE

Depending on the working and environmental conditions of the turbine location, the production characteristics of the turbine are different. Certain properties of turbines are widely used Here, wind turbines are divided into two groups according to their installation, whether in the sea Or in a righteousness In addition, depending on the platform type, wind turbines float. in the sea It is divided into a Split Fixed. Regarding the rotor rotation axis, the turbines are divided into two horizontal and vertical groups. Today, turbines used in the wind industry are mainly horizontal wind turbines. This is because the rotor of the horizontal wind turbine is located on the ground and benefits more from the wind, the profile of the wind above the ground is smoother. Otherwise, the vertical axis wind turbine is a less powerful turbine adapted to where the wind is unstable and close to the ground. The tower is the carrier element of the turbine and is designed according to the weight of the turbine to be placed there. Tower types are network and hybrid types for powerful small turbine and windmill applications. The tubular body tower is used for commercial turbines with large turbine weight. The direction of the rotor also depends on the weight of the turbine. To prevent the use of wobble mechanisms in small turbines, the positioning of the wind rotor is used by the design of the cabin, which allows it to turn to the movement of the wind. In vast commercial turbines, using the direction of the rear wind rotor, it can directly satisfy the wind in the rotor and use the wind in the rotor more.

Even This time , Done Production of turbines New With different blades In size and shape , But in the study it was observed that three wind turbines blade in a cut Efficiency, and its powerful methods can absorb the coming winds in a way Excellent And explain the permeability of the wind. Vertigo. Adjust the energy by tuning And adjust The speed of rotation of the blades at different wind speeds. The most used energy modification method for large turbines depends on the angle of inclination of the control sled. Because of its economy, controlling procrastination is the preferred method for turbines Less big The driver transmits strength. Cipher rotation To the generator.

Fig 2.4 shows the main components just now Rabinat Wind with three commonly used blades on the horizontal axis. The turbine contains control on the field, tube tower structure and transmission And the rest of the ingredients as P shape .

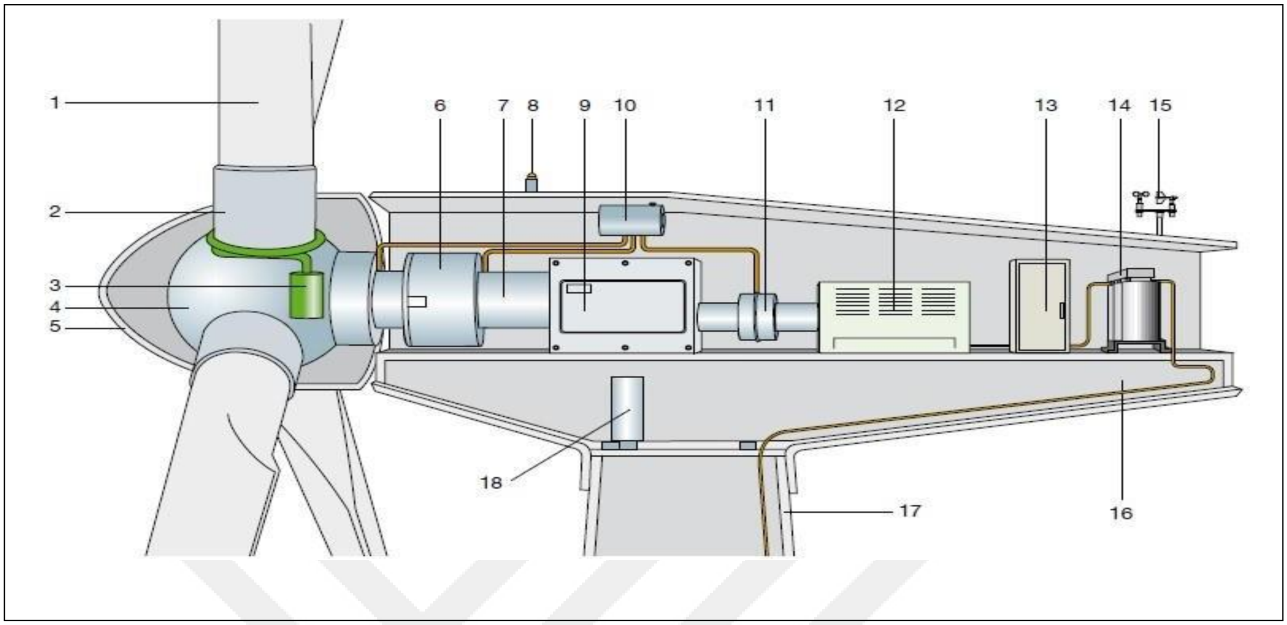

Figure 2.4: Main Components of wind turbine [16]

2.3 OFFSHORE WIND CONDITION

The environmental load at sea mainly consists of winds, waves and existing interactions, and even floating ice in the oceans of certain areas. Therefore, the design of turbines and platforms is done by examining whether they are affected by them. Figure 2.5 shows the outlines of wind and current and the waves schematically drawn in two dimensions. The current sea speed is displayed as a zero-background profile and increases the speed when it reaches the surface of the water . Otherwise, the wind profile has a speed of not sliding down on the sea surface that increases rapidly with height. Likewise, the wave load in the fig appears as a charge with its frequency and capacity between the current and wind reaction.

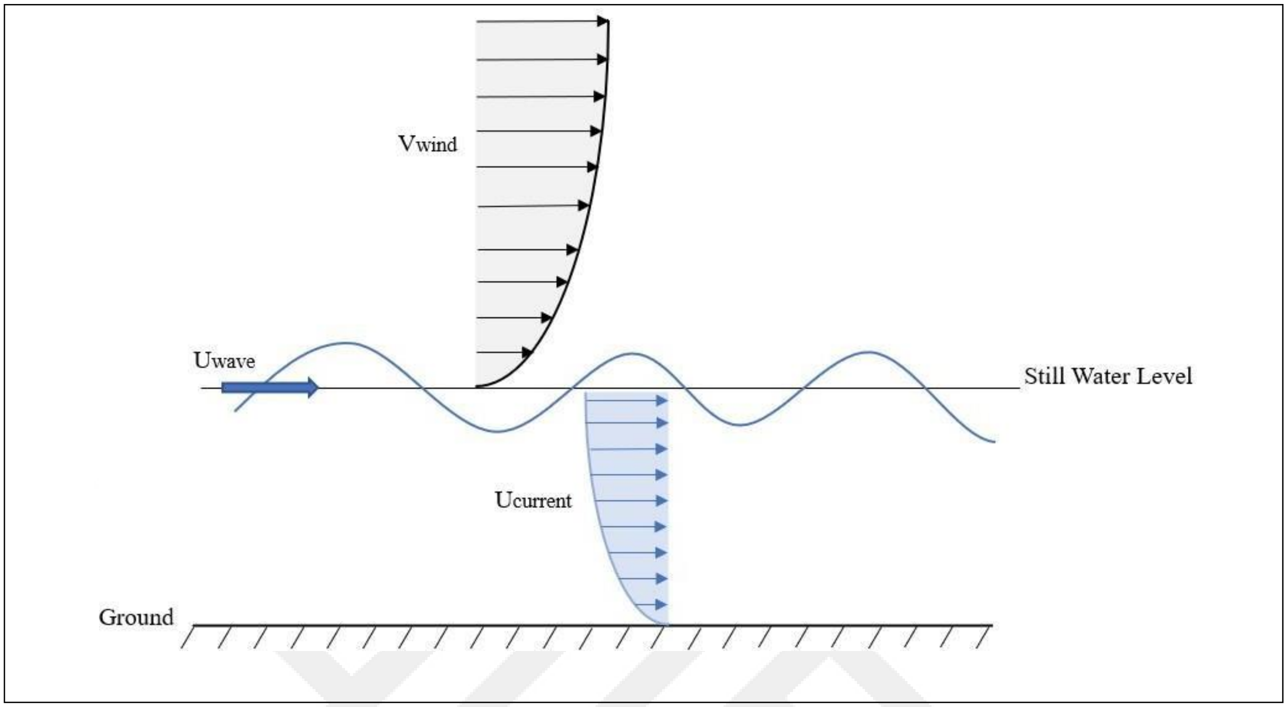

Figure 2.5: Environmental Loads

The current, wave and wind loads should not be in the same direction and every load is affected. Thus, changing the hierarchy of the wind profile, changing the profile gradient, and changing the frequency and amplitude of the wave depends on the atmosphere, weather and its interaction. Different sources of roughness (such as trees and structures on earth) will reduce the slope of the wind profile, so that the height of roughness increases and the potential for wind energy decreases to a certain height. By comparing the atmospheric boundary layers of the earth and the ocean, we can see that the profile of the wind formed in the ocean is smoother, so that the navel has an energy potential. Very high. It also means that the speed of the wind gradient is higher. Waves formed by the interaction of wind and waves form a rough surface in the ocean. The rough surface will affect the slope of the wind profile. If the wave and wind are in the same way the slope of the wind profile will increase; If the wind direction is different, the slope will decrease.[17] Using methods such as anemometers and satellites to process data collected over the years, the wind potential of the area can be removed. The calculated wind profile shows how to shape the atmospheric boundary in the area where the data is has been gotten. The representation of the instantaneous distribution of typical wind speeds is shown in Figure 2.6.

The actual wind speed difference shown in three-dimensional profile indicates that the flow is turbulent. The shift of the steep wind is displayed as a function of the average wind speed of the height increase.

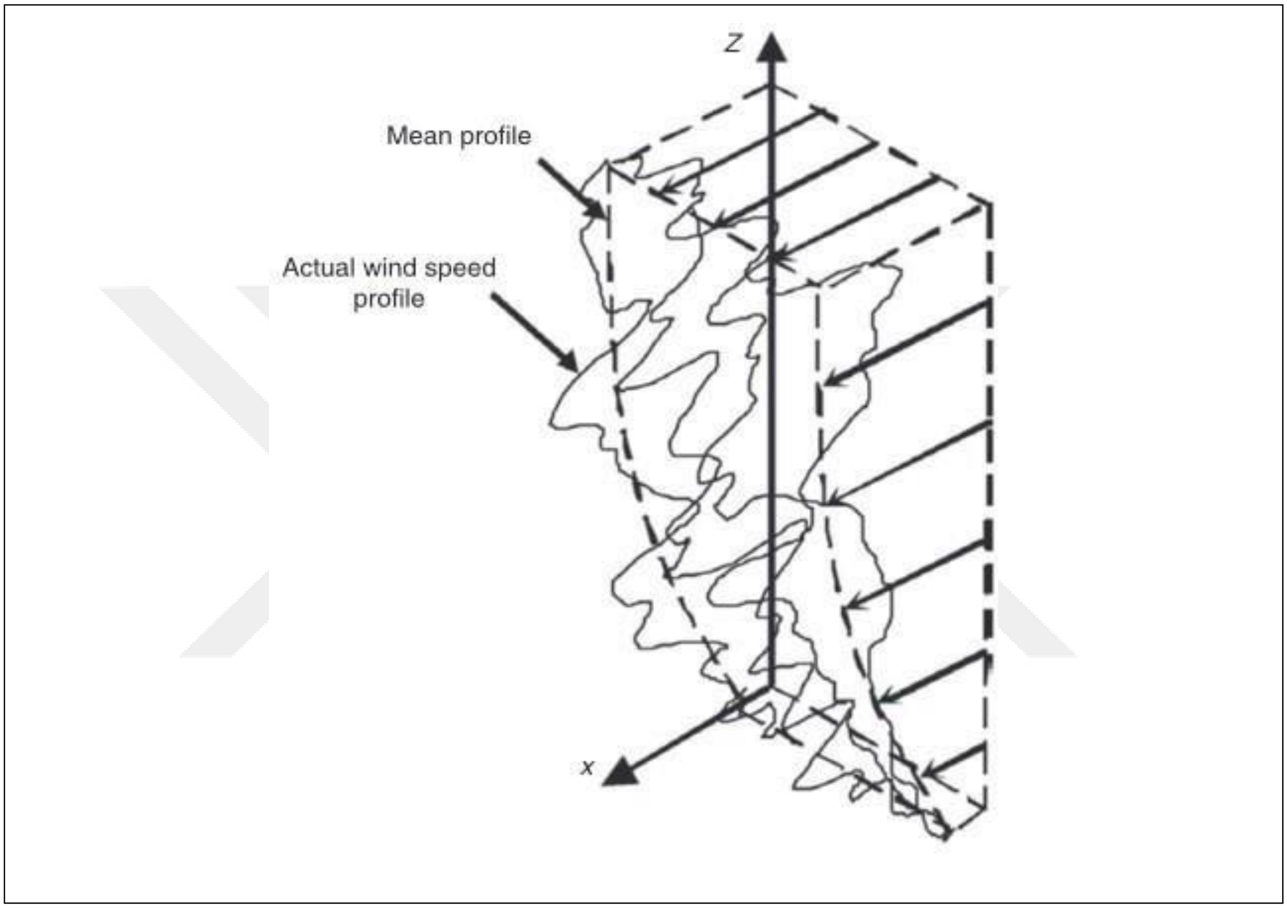

Figure 2. 6: Wind Profile [18]

3. MATERIAL AND METHOD

3.1 THE PARTICLE SWARM OPTIMIZATION { PSO }

Inspired by these studies, Kennedy and Eberhart introduced the Particle Swarm Optimization (PSO) or PSO algorithm in a paper in 1995. Particle swarm optimization algorithm or PSO algorithm is a "metaheuristic" algorithm that is suitable for optimizing nonlinear continuous functions. The authors of this paper have developed the PSO algorithm from the concept of Swarm Intelligence, which is commonly found in animal groups such as herds and flocks [19].

To make the general mechanism of the particle swarm optimization algorithm and other algorithms that are inspired by the group behavior of animals clearer, explanations about the group behavior (herd) of animals are provided. This explanation can help you understand how to build a particle swarm optimization algorithm (and other algorithms with a similar approach) [20].

A flock of birds moving over an area must find a point to land on. In this case, defining where all the birds should land is a complex matter. Because the answer to this question depends on various issues, ie maximizing the available food resources and minimizing the risk of predators at the landing point. In this situation, the observer can see the birds moving in the form of dancing. The birds move at the same time at a certain time to determine the best place to land and all the groups (groups) land at the same time [21].

In the example given about the movement of a flock of birds and their simultaneous landing, members of the flock (bird group) or the same flock of birds, have the opportunity to share information with each other. If the birds are not able to share information with each other in their own groups, each bird in the group (group) lands at a different place (point) and at a different time [22].

Research on bird behavior since the 1990s has shown that all birds in a swarm (group | group) looking for a good landing spot are able to get to the best landing spot when that spot is covered by A member of the crowd was found to be informed. Using this awareness, each member of the crowd balances their personal knowledge and crowd experience, known as "Social Knowledge" [23].

It is worth noting that the criteria used to evaluate whether a point is good or bad for landing are the survival conditions that will exist at one point for survival. These include the maximum food resources and the minimum risk of predators, which have been mentioned before [24].

To do this, each flying bird searches for a suitable landing spot and evaluates different points for different survival criteria to find the best landing area, and this is done until the best landing area is reached. Be determined by the total congestion [25].

Kennedy and Eberhart were inspired by the collective behavior of birds; Behavior that ensured significant survival benefits for the birds when searching for a safe landing spot. Accordingly, they developed an algorithm called the Particle Swarm Optimization algorithm. The PSO algorithm can mimic behavior similar to that of birds [26].

The purpose of optimization problems is to control the variable that is signified by the vector X = [x1, x2, x3, … , xn] and is maximized or minimized depending on the optimization formula provided by the function f (X). The inconstant vector X is known as a positive vector. This direction signifies a variable model and its n-dimensional vector, where n signifies the number of variables that might be specified in the problem. n is the latitude and longitude in finding the best place for a bird to terrestrial [27] and [28].

3.2 PSO COMPONENTS

The theory of employing a number of agents (particles, populations) that interact with simple natural methods to produce seemingly complex disability behaviors, to solve the problem of interpreting images in computer animations that tried to be similar to natural phenomena , Was used. Rios, one of the pioneers in this field, in part of his work at Lacasse Film, used particle devices, each consisting of a number of members working together to form a fuzzy function. The particle machine randomly generated a series of moving points, which typically began with predefined positions. In graphic simulation, there were other additional features such as color, texture and limited lifespan, and so on. The velocity vectors were repeatedly adjusted by some random factors. Then each particle, by adopting its velocity vector, detached from its current position and moved on to the next position. This location adjustment is done by taking a forced angle to make the move look realistic. Such systems were extensively developed to produce social outcomes and actual interactions of graphical environments. For some animations, it was necessary to present group behaviors with higher levels of dynamics than simple particles (such as a bird population). Creating a file initiating member behavior was possible but very tedious, and at the same time generating a response that seemed natural was difficult. Reynolds used the Rios particle system as the basis for his higher-level group algorithm. He considered the previous motion of particles and added to this motion other components such as inclinations, position recognition, and information correspondence. These additional behaviors of the group members followed the simple rules of being a group member, such as: members must avoid collisions, they must adapt their velocity vector to other members, and they must be in a better position than other members. The development of these basic models, while increasing the intelligence of individuals (members), eliminated the need for route registration. But increasing the level of autonomy of individuals causes problems such as incompatibility. Reynolds based a certain move on the priority of superiority, to solve the problem. But again, the decision can be completely indefinite and random. In a simple implementation, we might consider a device in which each particle is aware of the movements of the entire population that are taking place. In this case, with the increase in the number of population particles, the problem may become very complicated and even impossible. To solve this problem, Reynolds proposed the neighborhood system, which is also used in nature due to the limited visibility of members, although recent research suggests that this method changes the disabled behavior of the population. Kennedy and Haharat sought to extend Reynolds' model by reflecting social behaviors. More importantly, they replaced the simple goal of finding a nest developed by Hepner and Greenander, an algorithm developed from a periodic group algorithm, with a more realistic goal of finding food. This led researchers to use this algorithm for non-obvious mathematical problems. In these algorithms, the objective function of the problem is considered as a function of fitness for members of the population. (Which are now called representative because they are more general than the bird model). By removing the variables that were inefficient and redundant, a more efficient and simpler model was obtained [29][30]. The resulting algorithm for calculating the next particle position was expressed as follows:

$$v_{t+1}=v_t+\varphi_1\beta_1(p_i-x_i)+\varphi_1\beta_1(p_g-x_i) \qquad (3.1)$$

$$v_{i,k+1} = w * v_{i,k} + \alpha * r_1 * (PB - x_{i,k}) + \beta * r_2 * (GB - x_{i,k})$$

$$x_{t+1} = v_t + v_{t+1} \tag{3.2}$$

$$x_{i,k+1} = x_{i,k} + v_{i,k}$$

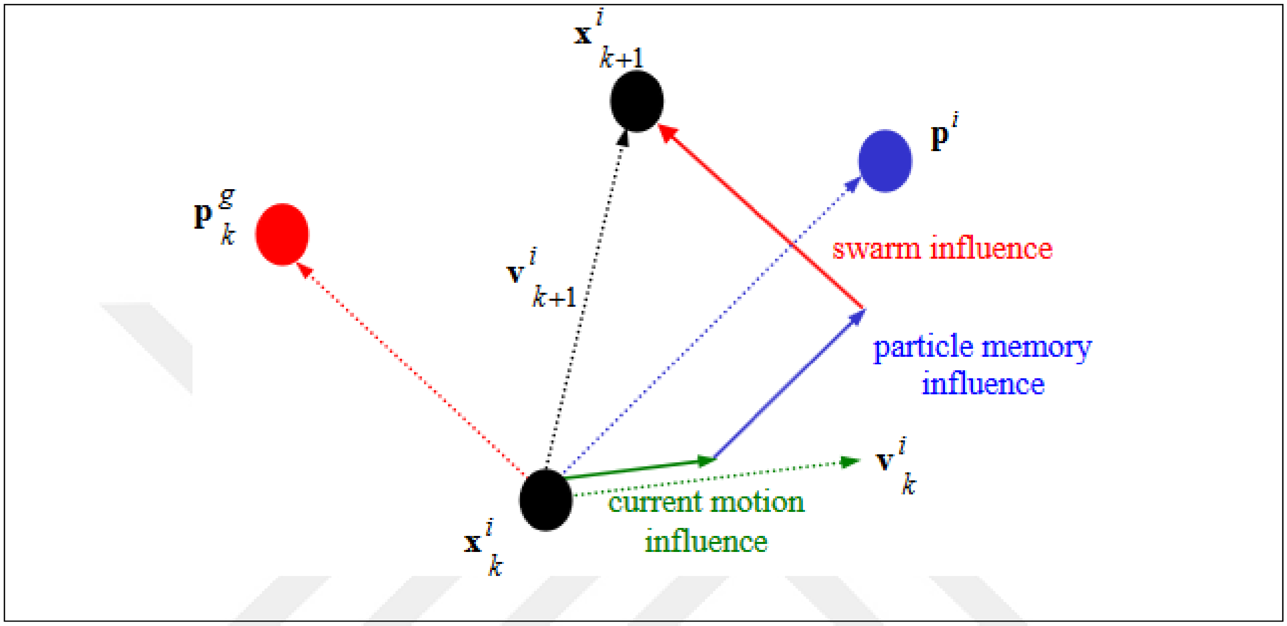

Figure 2.3: Velocity and Position Updates in PSO Diagram [31]

The parameters of PSO are shown in the Table 3.1, and the flowchart of it is shown in Figure 3.1 which it shows how the algorithm operates.

Table 3. 1: The Parameters of PSO

Parameter	Value
Maximum iteration (generation)	100
Population size of the swarm	24
Cognitive parameter	1.5
Social parameter	2
Constriction factor	1
Dimension of the problem	4

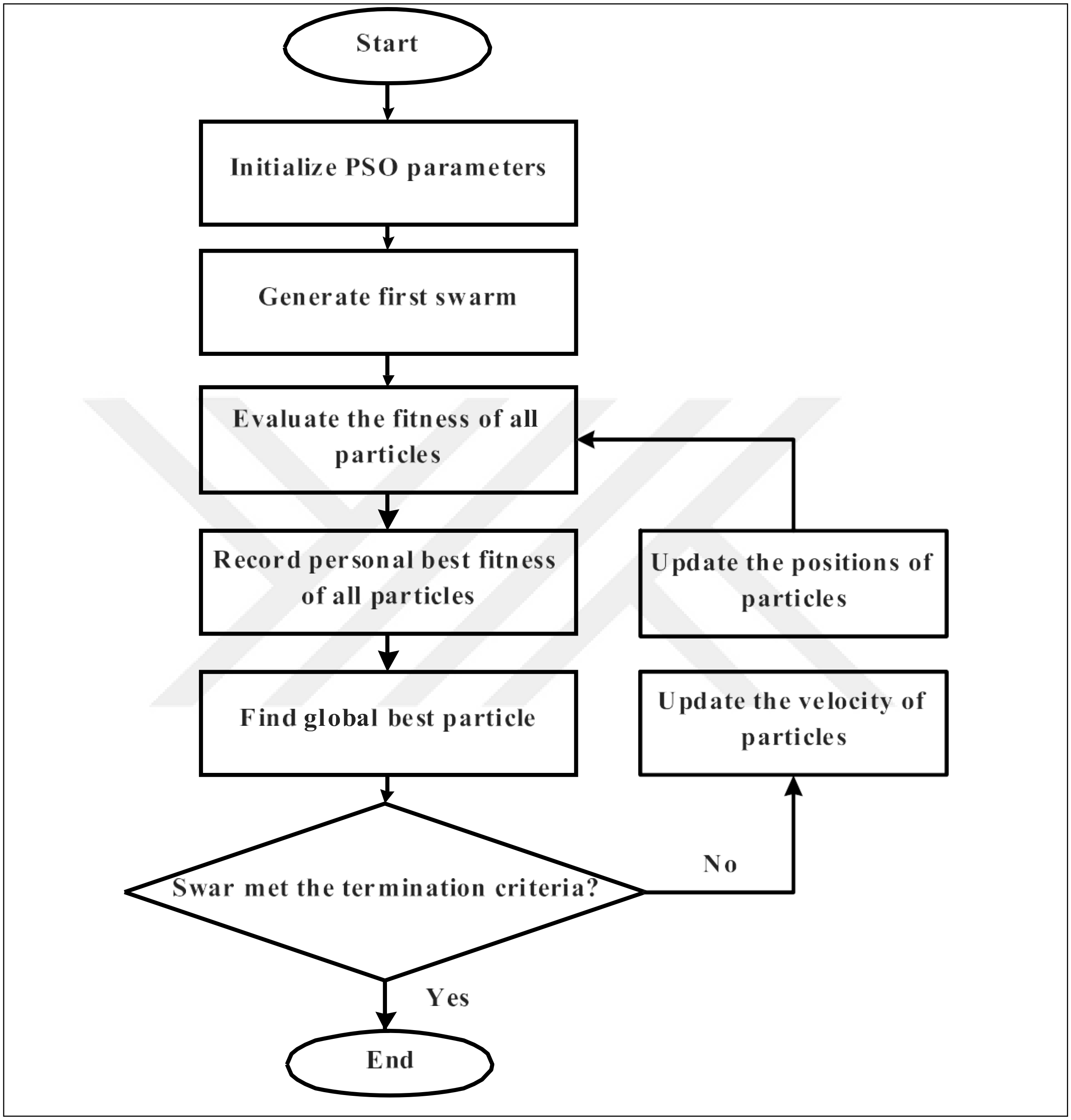

Figure 3. 1: PSO Flowchart

The Objective function against of the iteration is shown in figure 3.2.

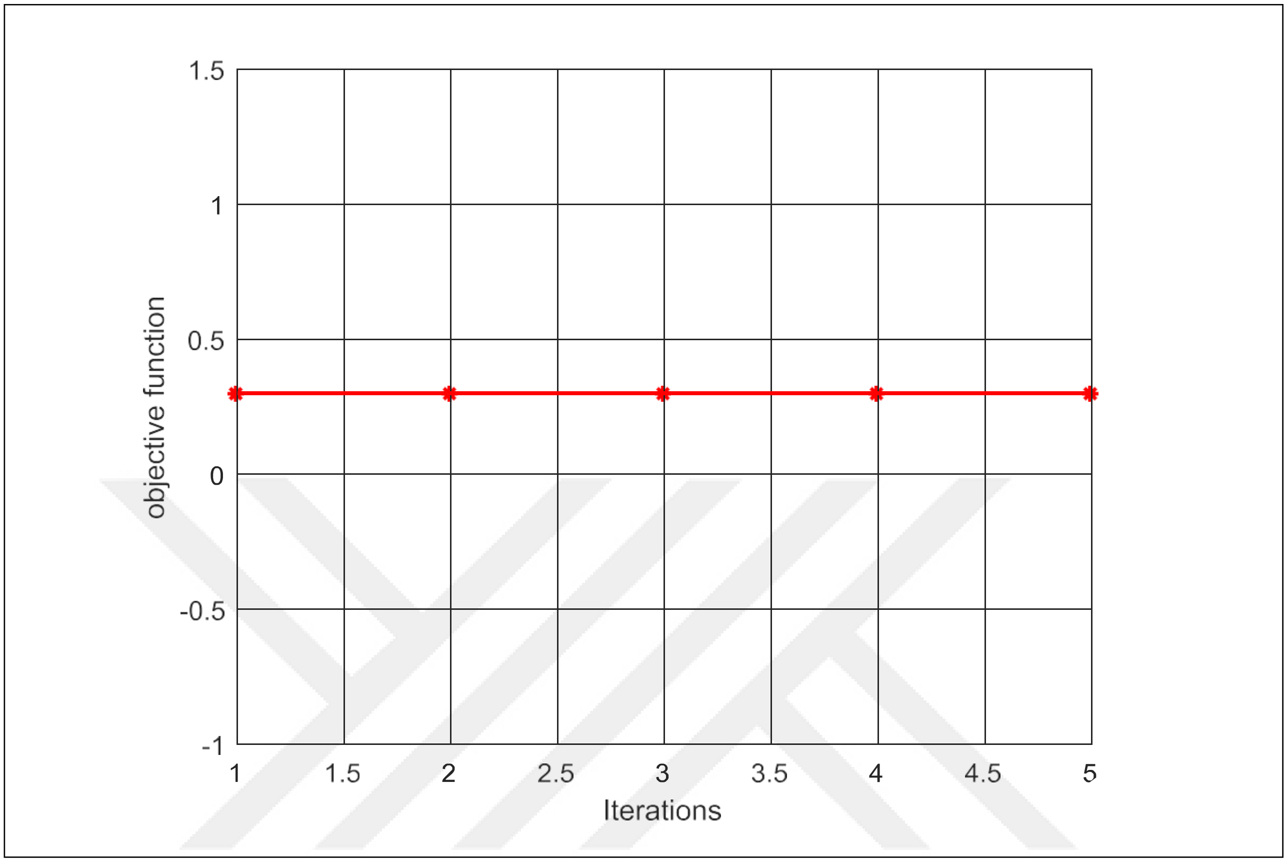

Figure 3.2: Objective Function against of the iteration

4. EXPERIMENTAL RESULTS AND DISCUSSION

4.1 GRID CONNECTED PMSG WIND GENERATOR

Normally PMSG wind energy connected with Grid system are classified as following, back-to-back connected PWM converter-based grid connected system and AC to DC and DC to AC converter-based grid connected system. Direct axis – Quadrature axis (d-q) vector control scheme and generator feed forward control scheme are normally used in the Grid connected PMSG wind energy system with back-to-back connected PWM converter. In this work, PID controller in the generator side control is optimized using Genetic Algorithm (GA) [32], PSO [33] and Grey Wolf Optimization (GWO) [34].

Diagram of the Block of Grid connected PMSG wind generator with back-to-back PWM converter system shown in Fig 4.1.

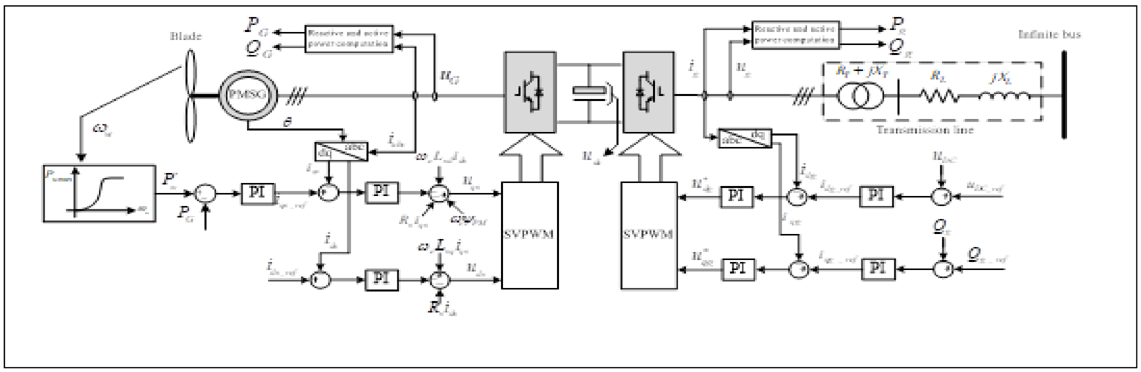

Figure 4.1: Block Diagram of the Grid connected PMSG wind generator with back-to-back connected PWM converter system

The system consists of the PMSG wind generator, controlled AC to DC converter, DC link capacitor, DC to AC converter, generator side control, grid side control and grid system. In the generator side control, wind speed is measured using speed sensor and it is converter into wind power (P_W). The wind power is compared with actual electrical power of the PMSG wind generator (P_G). The comparator output is processed via Proportional Integral Controller (PID) and provides reference quadrature current (i_{qs_ref}) for next stage. In the next stage, actual three phase current (i_a, i_b, i_c) of the PMSG is converted in to d-q axis current using Park transformation and it is represented by the following equation,

$$\begin{bmatrix} i_d \\ i_q \\ 0 \end{bmatrix} = \frac{2}{3} \begin{bmatrix} sin(\theta) & sin(\theta - \frac{2\pi}{3}) & sin(\theta + \frac{2\pi}{3}) \\ cos(\theta) & cos(\theta - \frac{2\pi}{3}) & cos(\theta + \frac{2\pi}{3}) \\ \frac{1}{2} & \frac{1}{2} & \frac{1}{2} \end{bmatrix} \begin{bmatrix} i_a \\ i_b \\ i_c \end{bmatrix} \quad (4.1)$$

In the next stage, the actual d-q axis current (i_{ds} & i_{qs}) is compared reference d-q axis current and it processed via Proportional Integral Controller. The Proportional (P) controller provides stator flux linkage ($\dot{\psi}_{ds}$ & $\dot{\psi}_{qs}$) for next stage. In the next stage, d-q axis voltages (u_{ds} & u_{qs}) are produced for generating gating pulse for the machine side PWM converter. The d-q axis voltage is represented by the following equation,

$$\begin{cases} u_{ds} = -R_s i_{ds} - \omega_r \psi_{qs} + \dot{\psi}_{ds} \\ u_{qs} = -R_s i_{qs} + \omega_r \psi_{ds} + \dot{\psi}_{qs} \end{cases} \quad (4.2)$$

The actual flux linkage for d-q axis is given by the following equation,

$$
\begin{cases}
\psi_{ds} = -L_{sd} i_{ds} + \psi_{rd} \\
\psi_{qs} = -L_{sq} i_{qs} + \psi_{rq} \\
\psi_{rd} = \psi_{PM} \\
\psi_{rq} = 0
\end{cases}
\tag{4.3}
$$

In the next stage, d-q axis voltages are converted in to reference a-b-c axis voltages with inverse estate transformation and it is represented by the following equations,

$$
\begin{bmatrix} u_a \\ u_b \\ u_c \end{bmatrix} = \frac{2}{3} \begin{bmatrix} \sin(\theta) & \cos(\theta) & 1 \\ \sin(\theta - \frac{2\pi}{3}) & \cos(\theta - \frac{2\pi}{3}) & 1 \\ \sin(\theta + \frac{2\pi}{3}) & \cos(\theta + \frac{2\pi}{3}) & 1 \end{bmatrix} \begin{bmatrix} u_d \\ u_q \\ 0 \end{bmatrix}
\tag{4.4}
$$

This reference a-b-c axis voltage is compared with triangular waveform to generate the PWM pulses for the machine side PWM converter. The performance of this machine side PWM converter is depends on the gain parameter of the d-q current processing Proportional (P) controller and this gain parameter is tuned using GA, PSO and GWO algorithm.

In grid side control, actual dc link voltage and reactive power has been compared with reference dc link voltage and reactive power setting. The output from the compared is processed via Proportional Integral (PI) controller and it is produces reference d-q axis current for next stage. In next stage, reference d-q axis current is compared with actual d-q axis current and it is processed via Proportional Integral (PI) controller and it produces d-q axis voltage. This d-q axis voltage is converted into a-b-c voltage quantity using inverse park transformation. This a-b-c voltage quantity is processed via sinusoidal PWM generator for generating gating pulses for generator side PWM converter. The overall Simulink model of connected PMSG wind generator with back-to-back connected PWM converter system is shown in Figure 4.2.

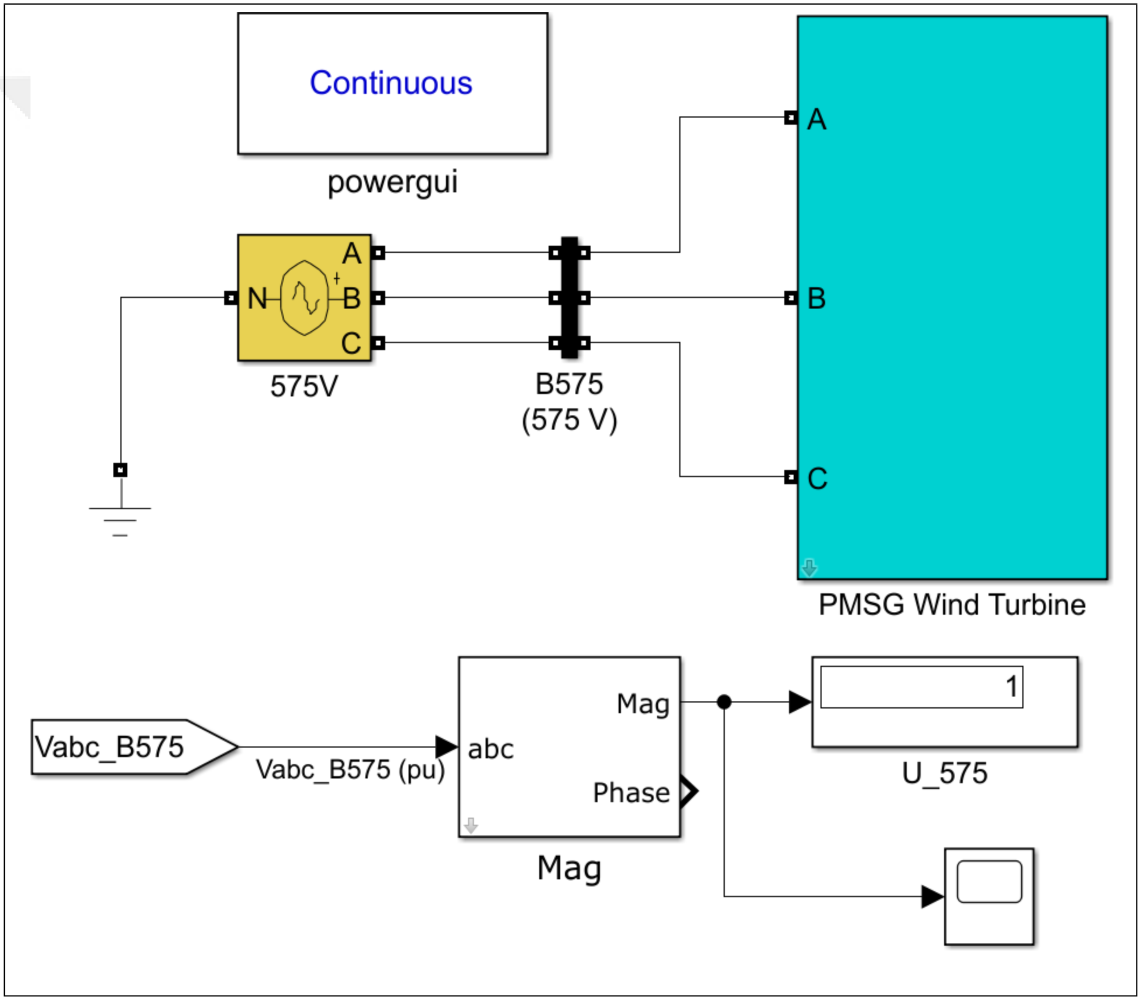

Figure 4.2: Simulink Model of connected PMSG wind generator with back-to-back connected (PWM) converter system

The Simulink model of measurement system is shown in Fig 4.3. In measurement and transformation system, voltage, current, speed, frequency, power and reactive power are measured in a-b-c quantity. These a-b-c quantities are converted in to d-q quantities using park transformation. And these quantities are used in grid side and machine side control system for generating pulses for PWM converter.

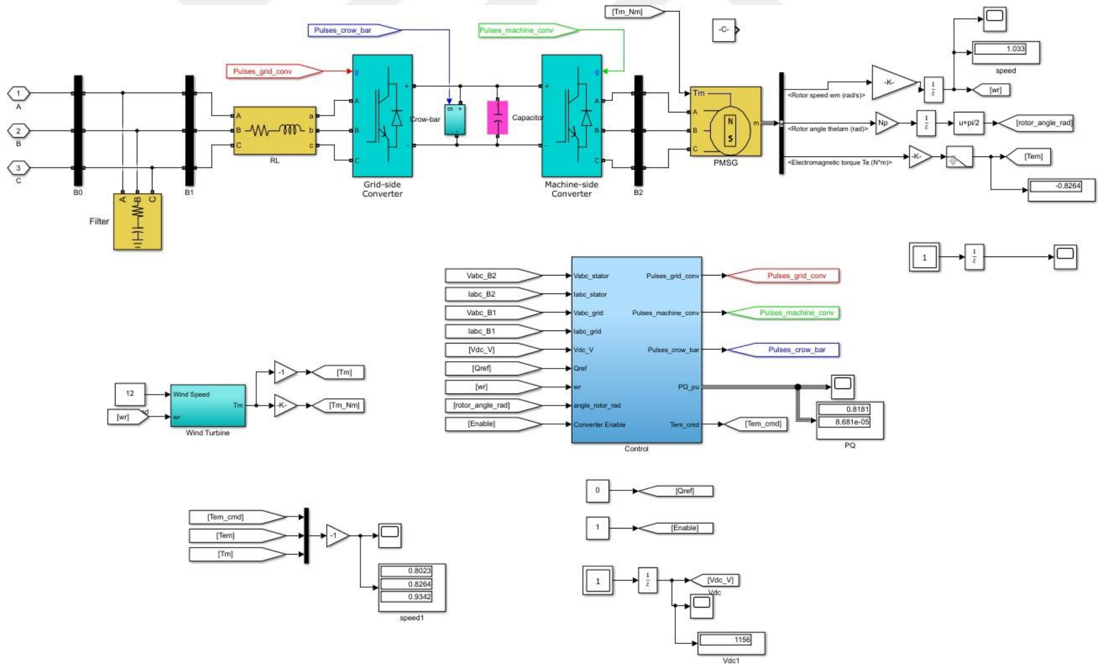

Figure 4.3: Simulink Model of the measurement and transformation system

The Simulink model of machine side control system shown in Fig 4.4.

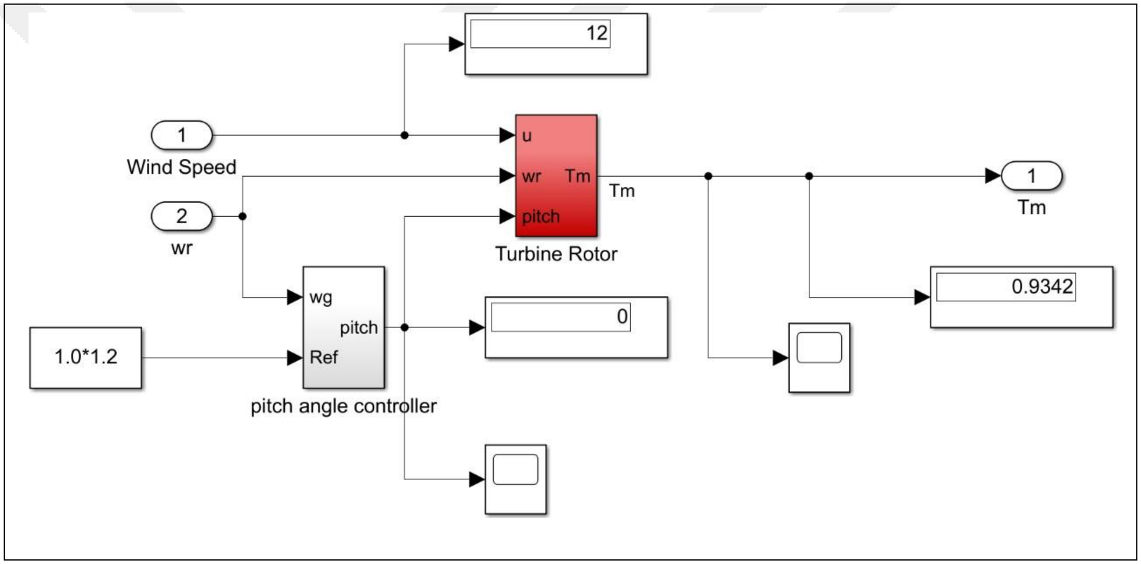

Figure 4.4: Simulink Model of the machine side control system

In this control system have two PI controllers for processing d-q axis currents. The parameter of the controller such as K_p, K_i, K_{p1} *and* K_{i1} are optimized using GA, PSO and GWO. The Simulink model of grid side control system shown in Fig 4.5.

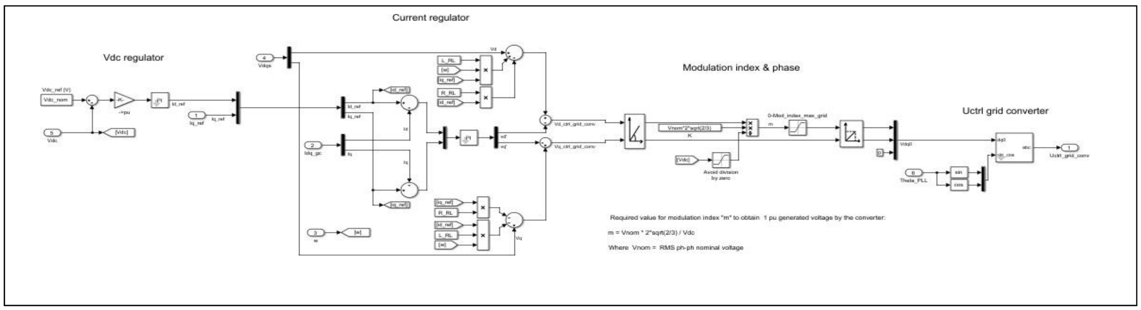

Figure 4.5: Simulink Model of grid side control system

The output result from Matlab is shown in figure 4.6.

```
      iter        Kp         Kp1        Ki         Ki1        Jmin
         0    0.0426    0.0197    0.0472    0.0240    0.4478
ErrorInEachPopulation =
    0.4478    0.7413
==============================================================
      iter        Kp         Kp1        Ki         Ki1        Jmin
    1.0000    0.0500    0.0500    0.0500    0.0500    0.2990
ErrorInEachPopulation =
    0.2990    0.2990
==============================================================
      iter        Kp         Kp1        Ki         Ki1        Jmin
    2.0000    0.0500    0.0500    0.0500    0.0500    0.2990
ErrorInEachPopulation =
    0.2990    0.2990
==============================================================
      iter        Kp         Kp1        Ki         Ki1        Jmin
    3.0000    0.0500    0.0500    0.0500    0.0500    0.2990
ErrorInEachPopulation =
    0.2990    0.2990
==============================================================
      iter        Kp         Kp1        Ki         Ki1        Jmin
    4.0000    0.0500    0.0500    0.0500    0.0500    0.2990
ErrorInEachPopulation =
    0.2990    0.2990
==============================================================
      iter        Kp         Kp1        Ki         Ki1        Jmin
    5.0000    0.0500    0.0500    0.0500    0.0500    0.2990
ErrorInEachPopulation =
    0.2990    0.2990
==============================================================
optimal_solution =
    0.0500    0.0500    0.0500    0.0500
Best =
    0.2990
comuputation_time =
  341.9550
```

Figure 4.6: Result From MATLAB

Electrical speed of the permanent magnet synchronism generator (PMSG) (Per Unit) can be shown as following equations:

$$\omega_{epu} = \frac{\omega_e}{\omega_s}$$

$$\omega_{epu} = \omega_m * \left(\frac{N_P}{\omega_s}\right)$$

$$\omega_s = 2 * \Pi * F_{nom}$$

Where, ω_m is the mechanical speed of the PMSG, ω_e is the electrical speed of the PMSG, ω_s is the synchronous speed of the PMSG, N_P is the number of pole pair of the PMSG, F_{nom} is the normal frequency of the grid system and it is taken as 60 Hz.

Simulink Block of this model is shown in fig 4.7.

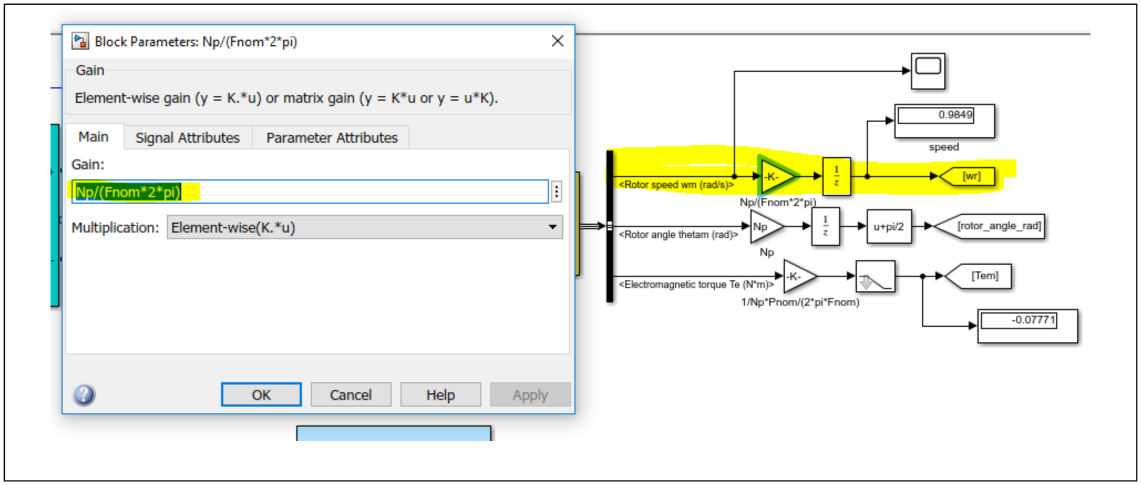

Figure 4.7: Simulink Block of the model

The Simulink model of the Electrical rotor angle of the PMSG (Actual) is shown in fig 4.8.

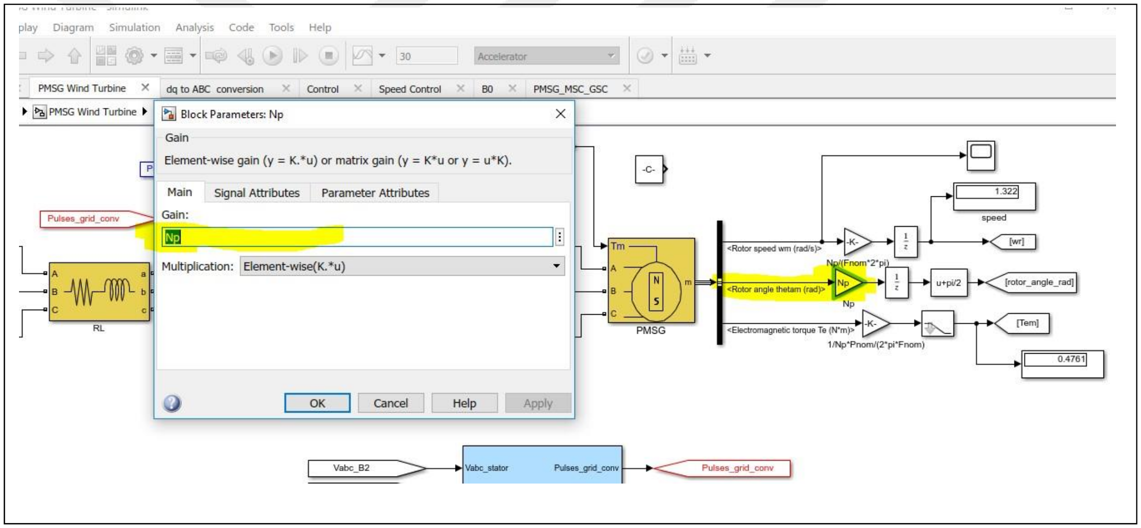

Figure 4.8: Simulink Model of the Electrical rotor angle of the PMSG

Relation between Torque, speed and power of the machine is shown in following equation.

$$T_d = \frac{\text{Mechanical power developed}}{\text{Mechanical angular velocity of the rotor}} = \frac{P_{md}}{\omega_r}$$

Electric magnetic Mechanical Torque PMSG (Per unit) is:

$$Te_{pu} = \frac{2 * \Pi * Fnom}{N_P * P_{nom}} T_e$$

Where, Te is the actual electromagnetic torque of the PMSG, Pnom is the normal rating of the wind energy adaptation system i.e., power assessment of the wind turbine.

Electrical Load Profile

Initially the load switch in off condition, during this time 1.5 MW load is connected with grid connected PMSG wind generator after 15 seconds, 0.75 MW load is added with grid connected PMSG wind generator. Test the system with variable load condition, this setup is created in the Simulink model that shown in figure 4.9.

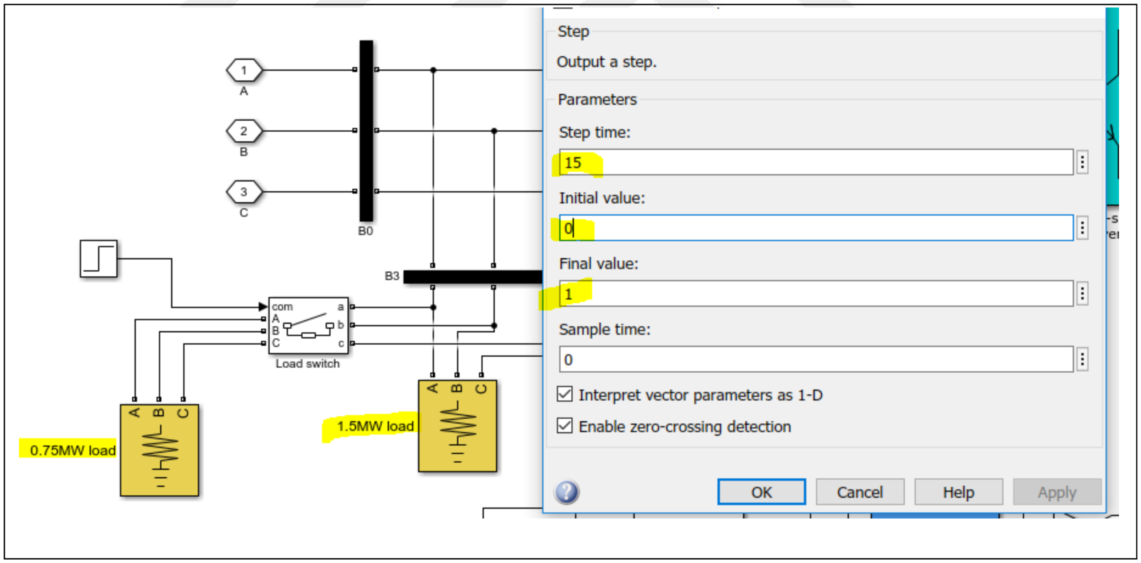

Figure 4.9: Test The System with variable load condition

Wind Turbine with Pitch angle control is shown in figure 4.10.

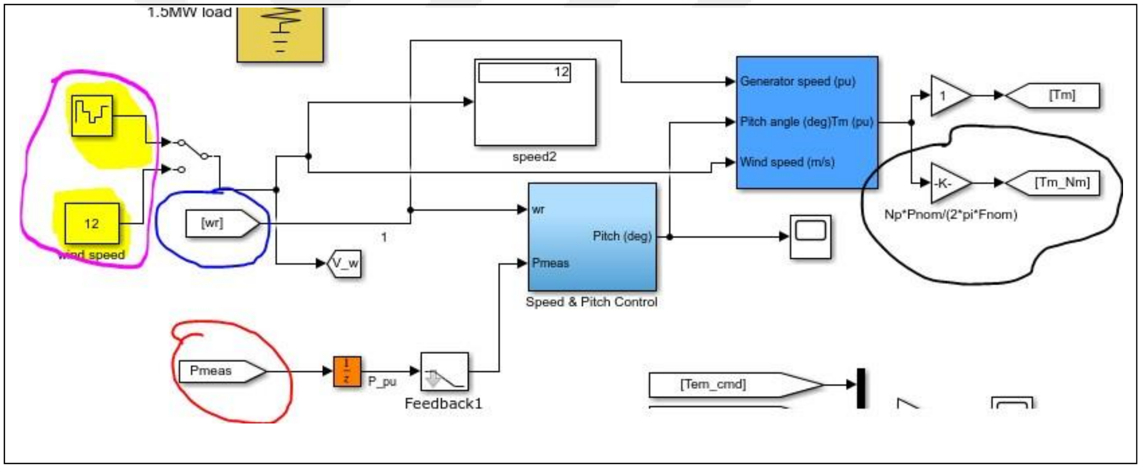

Figure 4.10: Wind Turbine with Pitch angle control

Pink color circle indicates the wind speed input for the wind turbine. Red color circle indicates the speed of the PMSG and this will act as input for both wind turbine and pitch angle control. Black circle indicate output from the wind turbine. This wind turbine supplies the per unit torque for PMSG and it should be converted in to actual torque for PMSG by using following equation,

$$T_m = \frac{N_P * P_{nom}}{2 * \Pi * Fnom} Tm_{pu}$$

The Pitch angle control is shown in fig 4.11.

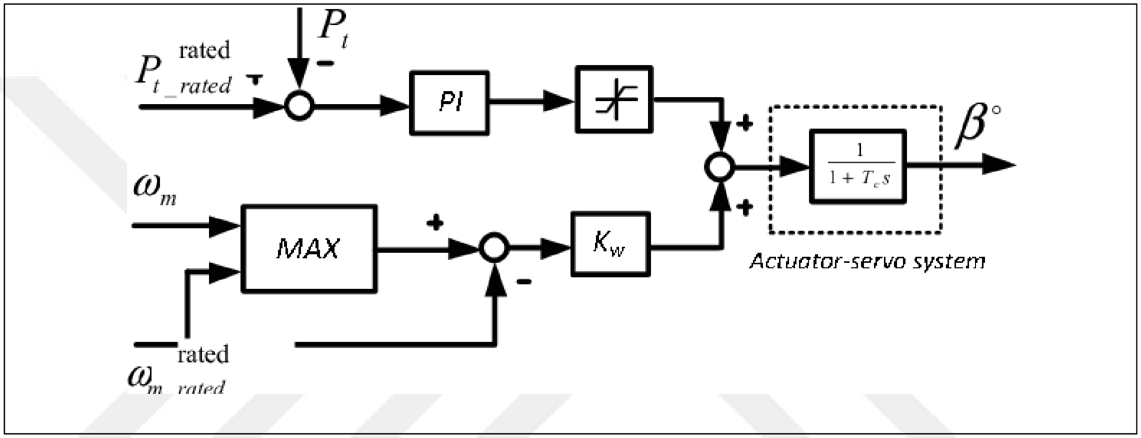

Figure 4.11: Wind Turbine pitch angle controller [35]

The Wind turbine model is shown in following equations:

$$P_t = \frac{1}{2} \rho A C_p(\lambda, \beta) v_w^3$$

$$T_t = \frac{1}{2} \frac{\rho R A}{\lambda} C_p(\lambda, \beta) v_w^2$$

$$\lambda = \frac{\omega_m R}{v_w}$$

$$C_p(\lambda, \beta) = c_1 \left(\frac{c_2}{\lambda_i} - c_3 \beta - c_4 \right) \cdot \exp\left(- \frac{c_5}{\lambda_i} \right)$$

$$\lambda_i = \left(\frac{1}{\lambda + 0.089} - \frac{0.035}{\beta^3 + 1} \right)^{-1}$$

The wind turbine data is shown in figure 4.12.

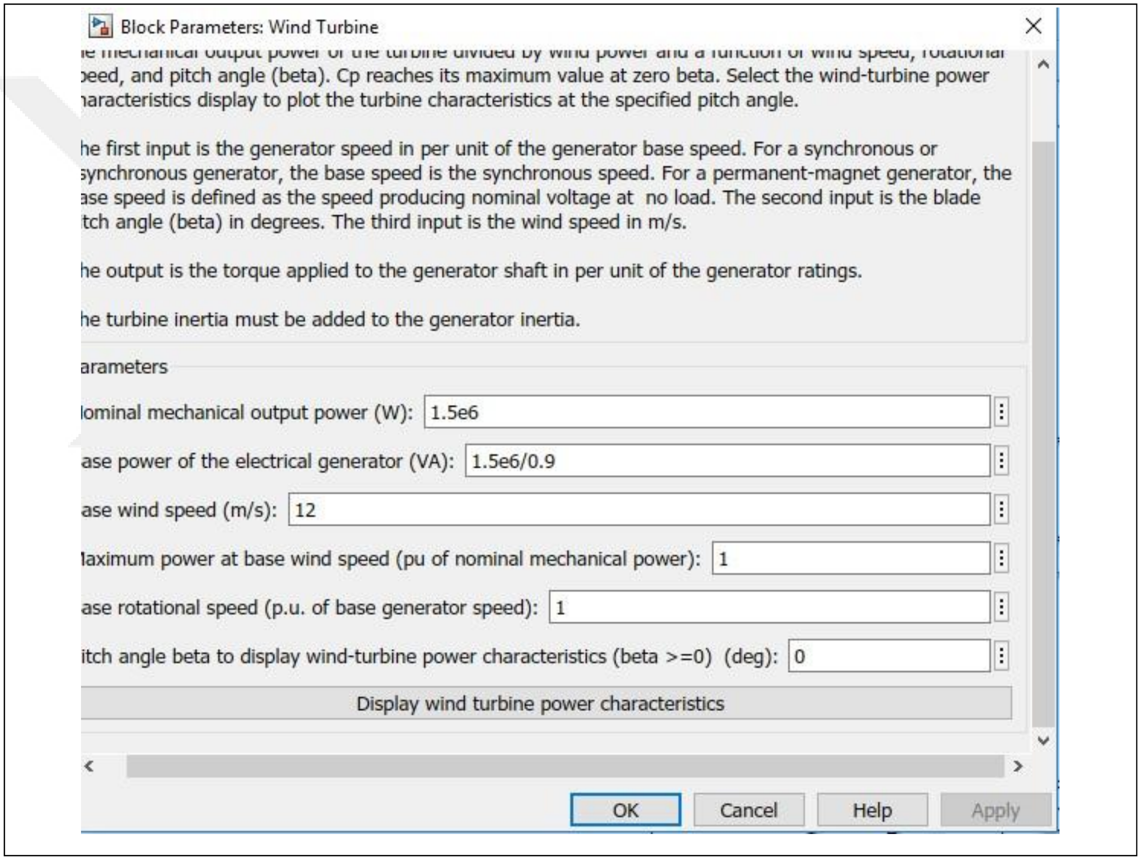

Figure 4.12: The Wind turbine data

The mechanical power of the turbine is 1.5 MW. Consider the efficiency o the wind turbine is 90 % then power at PMSG is 1.66 MW. Base wind speed is considered as 12 m/sec.

Graph for turbine speed, turbine output power with wind speed. The blue color line shows the maximum power point line for the wind turbine for different wind speed.

Red circle in this simulink model indicate the equation (1) and blue circle in the simulink model indicate the equation (4).

The machine side control and grid side control is shown in figure 4.13.

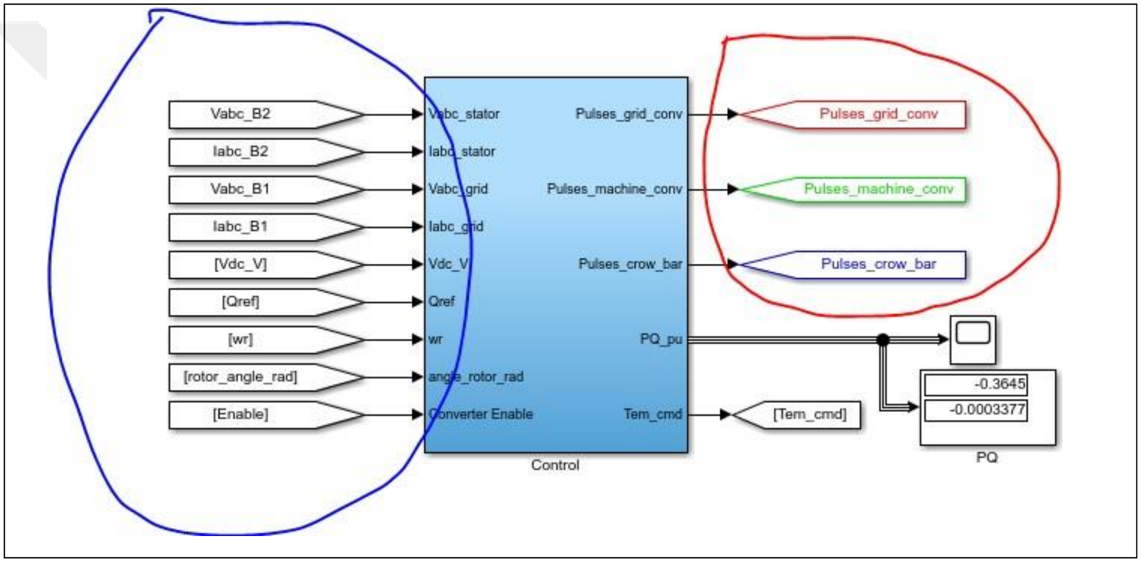

Figure 4.13: The Machine side control and grid side control

Control block receive the input from the grid connected PMSG wind energy system.

Input for this block is,

Bus bar 2 voltage and current i.e., PMSG terminal voltage and current drawn from the PMSG (Vabc_B2 and Iabc_B2).

Bus bar 1 voltage and current i.e., Grid side converter voltage and current (Vabc_B1 and Iabc_B1)).

Dc link voltage between machine converter and grid side converter (Vdc_V).

Speed and rotor angle of the PMSG (wr and rotor_angle_rad). And reactive power requirement (Qref) and it is normally set as zero because PMSG wind energy system always supply real power to grid. Enable input and it is always set to 1.

The output of this block is,

Gating Pulses for machine side converter (Pulses_machine_conv).
Gating pulses for grid side converter (Pulses_grid_conv).
Pulse for crow bar (Pulses_crow_bar) i.e., it is used to isolate the system when DC link voltage goes more than 1500 volts.

Blue circle in this simulink known as input for the block and red circle in this simulink known as output.

Filtering and Measurement system:

In this block, filter used to filter out the unwanted noises in the voltage, and the current, and the speed and rotor angle of the grid connected of PMSG wind energy structure. Red circle indicates the input for this Simulink block. Blue cycle indicates the output of this block. The output is dq voltage and current of the stator of the PMSG (Vdq_S and Idq_S), dq voltage and current of the grid side converter (Vdq_g and Idq_g), dc link voltage (Vmeas), generated power of the PMSG (Pmeas), reactive power of the PMSG (Qmeas) speed of the PMSG (wr), per unit frequency (w), angle difference between phases (Theta_PLL), rotor angle (r_angle_transform) and reference reactive power settings (Qref).
The Phase locked loop model is shown in figure 4.14.

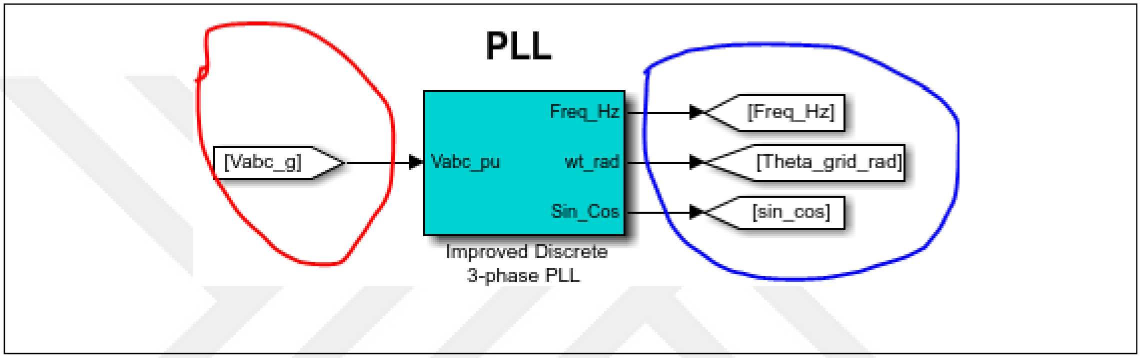

Figure 4.14: The Phase Locked loop model

The phase locked loop used for finding frequency of the grid side converter (Freq_Hz), phase difference between voltages (Theta_grid_rad), sin and cos component from the grid side voltage (sin_cos). Input for this block is grid side voltage(Vabc_g). This block used for real and reactive power calculation at bus bar 1, grid B575 and load bus using voltage and current of the corresponding bus. In this block per unit voltage and current is converted in to actual voltage and current. Formula for actual voltage and current conversions is shown below,

$$V_{abc(actual)} = V_{nom} * \frac{\sqrt{2}}{3} V_{abc(pu)}$$

$$I_{abc(actual)} = \frac{P_{nom}\sqrt{2}}{V_{nom}\sqrt{3}} I_{abc(pu)}$$

Speed regulator:

This block receives the speed of the PMSG (wr) and wind speed (V_w) and the output of the block of the q axis current reference (iq*)

Sub block of the speed regulator. Red circle indicate the MPPT using optimal tip speed ratio concept. Blue circle indicate the speed controller. The output of the controller provide reference q axis current for machine side control.

From the equation, speed required in rpm calculated by,

$$w_{rpm\_ref} = \frac{\lambda_{opt} * 60 * V_w}{\pi * D}$$

Rpm to rad/sec conversion,

$$w_{rad/sec} = w_{rpm} * \frac{6.283}{60}$$

The actual reference speed to per unit speed conversion,

$$\omega_{rad/sec_{pu}} = \omega_{rad/sec} * (\frac{N_P}{\omega_s})$$

$$\omega_s = 2 * \Pi * F_{nom}$$

The Crow bar protection model is shown in figure 4.15.

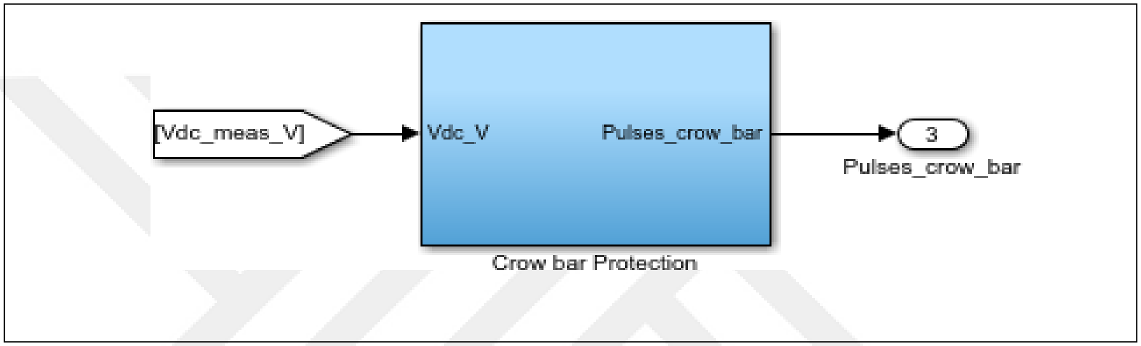

Figure 4.15: The Crow Bar protection model

The crow bar protection used to isolate the system when dc link voltage is more1500 volts to protect the system from over voltage.

This block inside the crowbar protection. Dc link voltage has been compared between 1500 to 1300. When dc link voltage is greater 1500 volt and pulse is in on condition and when dc link voltage is less than1300 volts and pulse is in off condition. The Machine Side control is shown in fig 4.16.

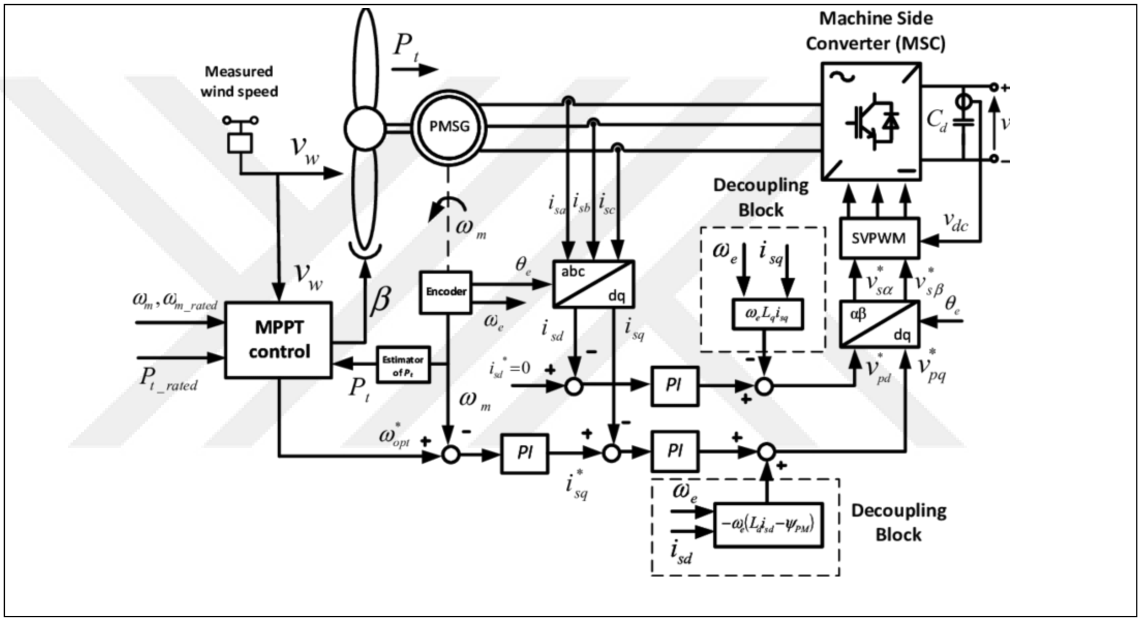

Figure 4.16: Control Diagram of the machine side converter [35]

In the red circle, actual direct axis current is compared with reference direct axis current and it is processed via PI controller. The output of the PI controller is added with flux linkage component. In the blue circle, actual quadrature axis current is compared with reference quadrature current and processed via PI controller. The output of the PI controller is added with flux linkage component. The actual output voltage Uds and Uqs is converted into per unit value by using following simulink block (see figure 4.17).

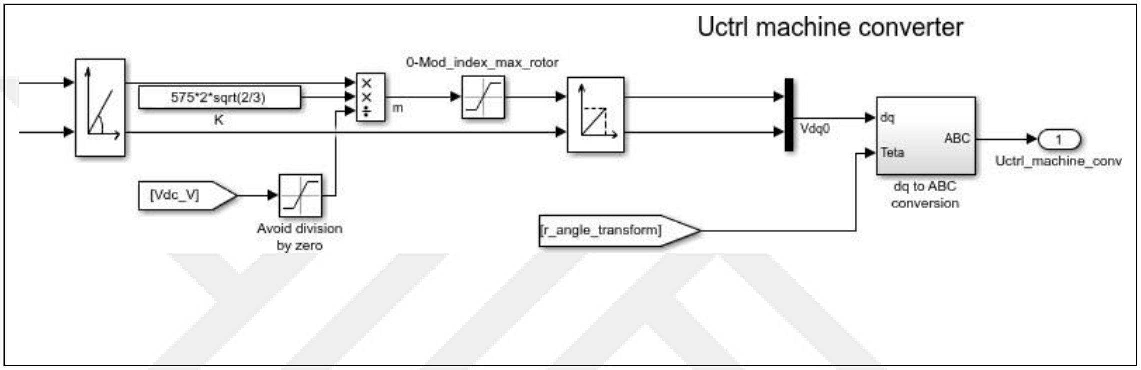

Figure 4.17: The Actual Output voltage Uds and Uqs is converted into per unit value

In this Simulink model, Cartesian coordinate voltage is converted in to polar coordinate voltage. After that is converted into per unit value by divided by the dc link voltage. After that it is converted into Cartesian coordinates voltages (Vdq0). Finally, dq voltage component is converting into abc voltage component by inverse transformation. The Grid side control shown in fig 4.18.

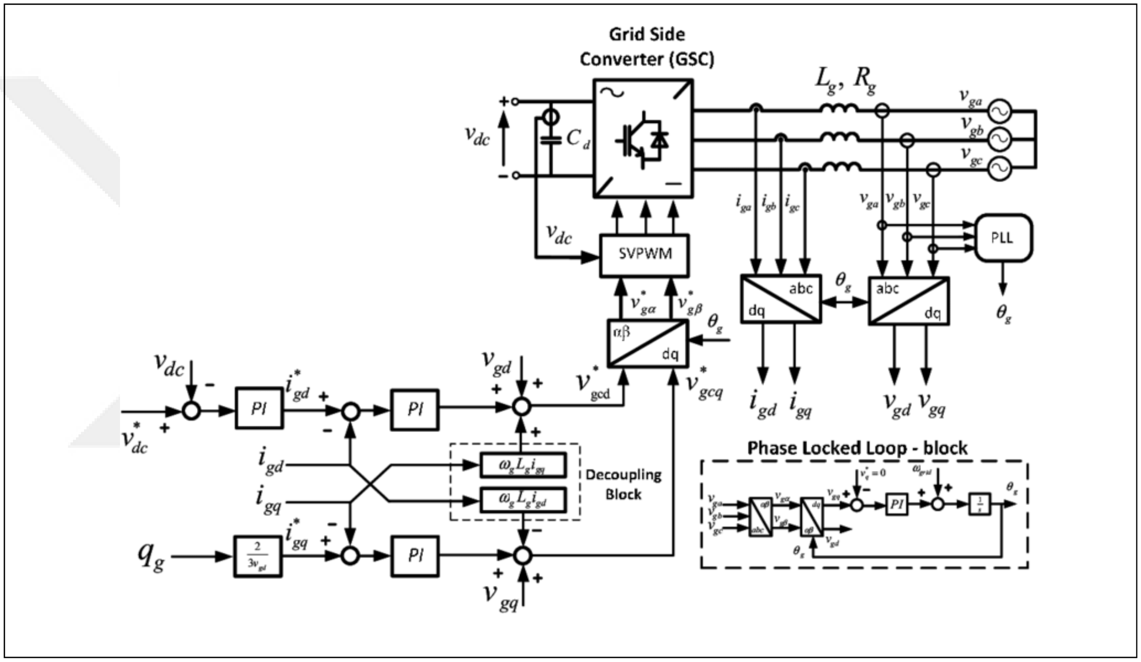

Figure 4.18: Control Diagram of the grid side converter [35]

The blue circle indicates the voltage regulator. In this regulator actual dc link voltage is compared with reference dc link voltage and processed via PI controller to generate the direct axis current reference. In this siumlink block, quadrature axis reference current is kept at zero i.e., PMSG only designed to supply real power only to grid. Red circle and pink circle indicates the current regulator. In this block, actual dq current is compared with dq actual current of the grid side and processed via PI controller. The output of the PI controller is added with flux linkage component to generate the dq voltage at grid side. That could be described by the equation, below .

$$
\begin{cases}
u_{gd} = U_{gd} + R_g i_{gd} + L_g \dfrac{di_{gd}}{dt} - \omega_e L_g i_{gq} \\
u_{gq} = U_{gq} + R_g i_{gq} + L_g \dfrac{di_{gq}}{dt} + \omega_e L_g i_{gd}
\end{cases}
$$

The actual output voltage Udg and Uqg is converted into per unit value by using following simulink block (See figure 4.19).

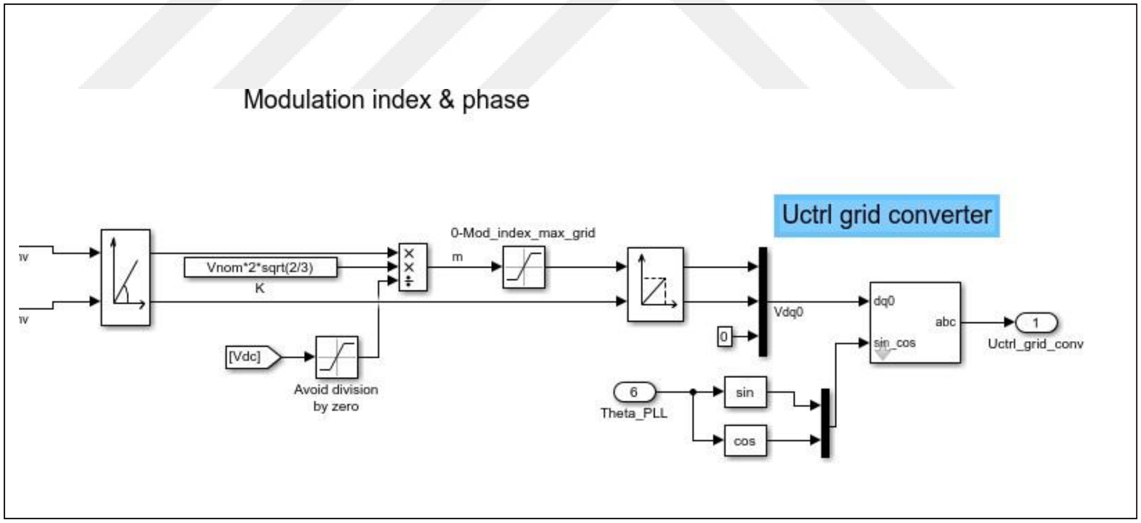

Figure 4.19: The Actual output voltage Udg and Uqg

In this Simulink model, Cartesian coordinate voltage is converted in to polar coordinate voltage. After that is converted into per unit value by divided by the dc link voltage. After that it is converted into Cartesian coordinates voltages (Vdq0). Finally, dq voltage component is converting into abc voltage component by inverse transformation.

5. CONCLUSION AND FUTURE WORK

5.1 CONCLUSION

Wind turbines can be used in combination in the form of clusters, so-called "wind farms" and are used by large companies to provide backup energy. In addition to the electrical energy mentioned above, this energy can be used to grind grains, pump water, charge batteries, and so on. The wind spins the turbine blades when it blows at a speed of about 3.5 meters per second. Also, the wind with a speed of 11 meters per second causes the maximum rotation of the turbines. When the wind is strong (25 meters per second), the turbine blades spin half-wheel and consequently the wind turbines slow down to prevent high voltage. The rotor is a three-bladed unit mounted in the middle of the turbine that rotates a slow axis connected to a gearbox or gearbox, increasing the rotation speed from 13 to 1500 rpm. In order to identify and eliminate any accidents, all important operations of wind turbines are monitored and managed from the control center and substation.

Wind power is one of the main types of renewable energies which have long occupied the human mind so that he has always thought about the use of this energy in industry. Humans have used wind energy to propel boats, yachts, and windmills. In the current situation, considering the mentioned cases and the economic justification of wind energy in comparison with other new energy sources, dealing with wind energy seems to be vital and necessary. Between sustainable power sources, the breeze energy is one of the furthermost prudent strategies for creating power that doesn't dirty the climate and is likewise boundless. As per accessible measurements, the creation of every kilowatt hour of electrical energy since the breeze can forestall the arrival of around one kilogram of CO_2 contrasted with petroleum product power plants. In general, greenhouse gas emissions can be reduced by replacing wind power with fossil fuel power plants. Wind energy, like other renewable energy sources, is geographically extensive, yet dispersed and decentralized and almost always available. Wind power is one of the main types of renewable energies whice have long occupied the human mind so that he has always thought about the use of this energy in industry. The energy supply market is a competitive market in which the production of electricity from wind farms compared to fossil fuel power plants has put new advantages in front of the energy sector. The extensive activity of a number of countries in the world to generate electricity from wind energy is also an example for other countries that have a long way to go in this field.

This simulation works concentrated speed control of PMSM using PI controller and powered by wind turbine system. The proposed model has been verified its performance under various operating condition.

Moreover, under wind irradiation level and ambient temperature change of wind turbine, PSO algorithm adjust the Vc as desired in order to set D for both modulation techniques.

With performing of this inspection, wind energy converted to electrical energy by wind turbine arrays and an MPPT method is used. In addition, the speed control of the PMSM is carried out through field-guided control and three-phase inverter structure. It is predicted to be very useful and efficient in applications such as water independent pumping systems and electric vehicles.

5.2 FUTURE WORK

As a future work, experimental set up of this study for grid isolated application such as water pump or electrical vehicle will be realized.

REFERENCES

[1] S. J. Ghoushchi, S. Manjili, A. Mardani, and M. K. Saraji, “An extended new approach for forecasting short-term wind power using modified fuzzy wavelet neural network: A case study in wind power plant,” *Energy*, vol. 223, p. 120052, 2021.

[2] M. Koivisto, K. Plakas, E. R. H. Ellmann, N. Davis, and P. Sørensen, “Application of microscale wind and detailed wind power plant data in large-scale wind generation simulations,” *Electr. Power Syst. Res.*, vol. 190, p. 106638, 2021.

[3] W. Zhou, Y. Wang, R. E. Torres-Olguin, and Z. Chen, “Effect of reactive power characteristic of offshore wind power plant on low-frequency stability,” *IEEE Trans. Energy Convers.*, vol. 35, no. 2, pp. 837–853, 2020.

[4] R. J. Barthelmie and S. C. Pryor, “Climate change mitigation potential of wind energy,” *Climate*, vol. 9, no. 9, p. 136, 2021.

[5] E. Möllerström, P. Gipe, J. Beurskens, and F. Ottermo, “A historical review of vertical axis wind turbines rated 100 kW and above,” *Renew. Sustain. Energy Rev.*, vol. 105, pp. 1–13, 2019.

[6] T. Zimmermann, M. Rehberger, and S. Gößling-Reisemann, “Material flows resulting from large scale deployment of wind energy in Germany,” *Resources*, vol. 2, no. 3, pp. 303–334, 2013.

[7] U. ELİBÜYÜK and İ. ÜÇGÜL, “Rüzgâr türbinleri, çeşitleri ve rüzgâr enerjisi depolama yöntemleri,” *SDÜ Yekarum e-Dergi*, vol. 2, no. 3, 2014.

[8] M. Ragheb and A. M. Ragheb, “Wind turbines theory-the betz equation and optimal rotor tip speed ratio,” *Fundam. Adv. Top. Wind power*, vol. 1, no. 1, pp. 19–38, 2011.

[9] Z. Yang, “Wind turbine controls for farm and offshore operation.” The University of Wisconsin-Milwaukee, 2013.

[10] S. P. Evans, D. R. Bradney, and P. D. Clausen, “Aeroelastic measurements and simulations of a small wind turbine operating in the built environment,” in *Journal of Physics: Conference Series*, 2016, vol. 753, no. 4, p. 42013.

[11] F. Castellani, D. Astolfi, M. Peppoloni, F. Natili, D. Buttà, and A. Hirschl, “Experimental vibration analysis of a small scale vertical wind energy system for residential use,” *Machines*, vol. 7, no. 2, p. 35, 2019.

[12] A. Das and P. K. Talapatra, “Modelling and analysis of a mini vertical axis wind turbine,” *Int. J. Emerg. Technol. Adv. Eng.*, vol. 6, no. 6, pp. 184–194, 2016.

[13] K. E. Johnson, “Adaptive torque control of variable speed wind turbines,” National Renewable Energy Lab., Golden, CO (US), 2004.

[14] R. M. Ochieng, F. N. Onyango, and A. O. Oduor, “Physical formulation of the expression of wind power,” *Int. J. Energy, Environ. Econ.*, vol. 18, no. 1, p. 107, 2010.

[15] P. M. Anderson and A. Bose, “Stability simulation of wind turbine systems,” *IEEE Trans. power Appar. Syst.*, no. 12, pp. 3791–3795, 1983.

[16] H. D. M. de Azevedo, A. M. Araújo, and N. Bouchonneau, “A review of wind turbine bearing condition monitoring: State of the art and challenges,” *Renew. Sustain. Energy Rev.*, vol. 56, pp. 368–379, 2016.

[17] B. Lange, S. E. Larsen, J. Hojstrup, and R. J. Barthelmie, “The wind speed profile at offshore wind farm sites,” in *Proc. of the OWEMES 2003 Conference, Naples (Italy)*, 2003.

[18] J. Van Der Tempel, “Design of support structures for offshore wind turbines,” 2006.

[19] J. A. Allen, “Community through culture: From insects to whales: How social learning and culture manifest across diverse animal communities,” *BioEssays*, vol. 41, no. 11, p. 1900060, 2019.

[20] V. Fernandez-Viagas, R. Ruiz, and J. M. Framinan, “A new vision of approximate methods for the permutation flowshop to minimise makespan: State-of-the-art and computational

evaluation," *Eur. J. Oper. Res.*, vol. 257, no. 3, pp. 707–721, 2017.

[21] G. Beni, "Swarm intelligence," *Complex Soc. Behav. Syst. Game Theory Agent-Based Model.*, pp. 791–818, 2020.

[22] B. H. Nguyen, B. Xue, and M. Zhang, "A survey on swarm intelligence approaches to feature selection in data mining," *Swarm Evol. Comput.*, vol. 54, p. 100663, 2020.

[23] W. Niu, Z. Feng, B. Feng, Y. Xu, and Y. Min, "Parallel computing and swarm intelligence based artificial intelligence model for multi-step-ahead hydrological time series prediction," *Sustain. Cities Soc.*, vol. 66, p. 102686, 2021.

[24] X.-S. Yang and S. Deb, "Cuckoo search: recent advances and applications," *Neural Comput. Appl.*, vol. 24, no. 1, pp. 169–174, 2014.

[25] K. E. Colson *et al.*, "Optimizing matching and analysis combinations for estimating causal effects," *Sci. Rep.*, vol. 6, no. 1, pp. 1–11, 2016.

[26] W. K. T. Cho, "An evolutionary algorithm for subset selection in causal inference models," *J. Oper. Res. Soc.*, pp. 1–15, 2017.

[27] X.-S. Yang, Z. Cui, R. Xiao, A. H. Gandomi, and M. Karamanoglu, *Swarm intelligence and bio-inspired computation: theory and applications*. Newnes, 2013.

[28] A. Barolli, S. Sakamoto, L. Barolli, and M. Takizawa, "Performance analysis of simulation system based on particle swarm optimization and distributed genetic algorithm for WMNs considering different distributions of mesh clients," in *International Conference on Innovative Mobile and Internet Services in Ubiquitous Computing*, 2018, pp. 32–45.

[29] J. J. Sauppe, *Balance optimization subset selection: A framework for causal inference with observational data*. University of Illinois at Urbana-Champaign, 2015.

[30] W. K. T. Cho and Y. Y. Liu, "A parallel evolutionary algorithm for subset selection in causal inference models," in *Proceedings of the XSEDE16 Conference on Diversity, Big Data, and Science at Scale*, 2016, pp. 1–8.

[31] R. Hassan, B. Cohanim, O. De Weck, and G. Venter, “A comparison of particle swarm optimization and the genetic algorithm,” in *46th AIAA/ASME/ASCE/AHS/ASC structures, structural dynamics and materials conference*, 2005, p. 1897.

[32] D. M. Mukhopadhyay, M. O. Balitanas, A. Farkhod, S.-H. Jeon, and D. Bhattacharyya, “Genetic algorithm: A tutorial review,” *Int. J. grid Distrib. Comput.*, vol. 2, no. 3, pp. 25–32, 2009.

[33] M. Clerc, *Particle swarm optimization*, vol. 93. John Wiley & Sons, 2010.

[34] S. Mirjalili, S. M. Mirjalili, and A. Lewis, “Grey wolf optimizer,” *Adv. Eng. Softw.*, vol. 69, pp. 46–61, 2014.

[35] P. Gajewski and K. Pieńkowski, “Advanced control of direct-driven PMSG generator in wind turbine system,” *Arch. Electr. Eng.*, vol. 65, no. 4, pp. 643–656, 2016.